



CONTRACT NO. A932-054
FINAL REPORT
OCTOBER 1992

LIBRARY
CALIFORNIA AIR RESOURCES BOARD
P.O. BOX 2815
SACRAMENTO, CA 95812

Modeling Aerosol Processes and Visibility Based on the SCAQS Data

CALIFORNIA ENVIRONMENTAL PROTECTION AGENCY



AIR RESOURCES BOARD
Research Division

**MODELING AEROSOL PROCESSES AND VISIBILITY BASED ON
THE SCAQS DATA**

**Final Report
Contract No. A932-054**

LIPPARDY
CALIFORNIA AIR RESOURCES BOARD
SACRAMENTO

Prepared for:

Research Division
California Air Resources Board
2020 L Street
Sacramento, California 95814

Submitted by:

Environmental Quality Laboratory
California Institute of Technology
Pasadena, California 91125

Prepared by:

Anthony S. Wexler
Annmarie Eldering
Spyros N. Pandis
Glen R. Cass
John H. Seinfeld
K.C. Moon
and
Suzanne Hering

October 1992

Executive Summary

The principal objective of this research program was determination of the equilibrium distribution of pollutant materials between the gas and aerosol phases and of the subsequent relationships between the ambient aerosol and resultant visibility deterioration in the South Coast Air Basin of California. The Southern California Air Quality Study (SCAQS) data base was used extensively in addressing these two issues.

Equilibrium Distribution of Volatile Salts Between Gas and Aerosol Phases

Stelson *et al.* (1979) proposed in 1979 that particulate ammonium nitrate levels in the atmosphere are determined by thermodynamic equilibrium among ammonia, nitric acid, and ammonium nitrate. Ambient measurements of ammonia, nitric acid, and nitrate prior to SCAQS (Hildemann *et al.* 1984; John *et al.* 1985; Jacob *et al.* 1986) were not sufficiently extensive to test in detail whether equilibrium truly exists for ammonium nitrate between gas and aerosol phases. This basic question is important because in a polluted urban environment, the ammonium salts NH_4NO_3 and NH_4Cl account for 10-30% of the fine aerosol mass, and accurate prediction of the quantity of ammonium salts in the aerosol phase and their distribution with respect to particle size is essential to a full understanding of the source-receptor relations that govern the formation of the atmospheric aerosol.

By evaluating the time scales for equilibration of the vapor-phase species with a population of aerosol particles, we have found that ammonium salts in the gas and aerosol phases are not always in equilibrium, especially under less polluted and cooler conditions. Thus, both transport and thermodynamic properties of the aerosol population govern the distribution of ammonium salts. The transport rate is governed by the phase state (liquid, solid, or liquid/solid) and composition of the aerosol. We have developed an aerosol inorganic model that assumes (1) thermodynamic equilibrium within the aerosol and between water in the gas and aerosol phases; and (2) transport of inorganics between gas and aerosol phases.

One of the most intriguing aspects of atmospheric aerosols concerns the behavior of ammonium nitrate. As noted above, Stelson *et al.* (1979) first suggested that aerosol ammonium nitrate levels could be determined from the equilibrium among ammonia, nitric acid, and aerosol ammonium nitrate. The assumption of thermodynamic equilibrium has been employed to partition the volatile compounds between the gas and aerosol phases (Bassett and Seinfeld, 1983; Russell *et al.* 1983; Saxena *et al.* 1983, 1986; Russell and Cass, 1986; Russell *et al.*, 1988) and to predict their aerosol size distribution

(Bassett and Seinfeld, 1984; Pilinis *et al.*, 1987; Pilinis and Seinfeld, 1987, 1988).

Although the equilibrium assumption has been supported by some ambient data (Doyle *et al.*, 1979; Grosjean, 1982; Hildemann *et al.*, 1984), other data indicate that it may not always hold (Cadle *et al.*, 1982; Tanner, 1982; Allen *et al.*, 1989).

In previous work we have predicted that under certain atmospheric conditions, the volatile inorganic components of atmospheric aerosol may not be in equilibrium with their gas-phase counterparts due to transport limitations, so that under such conditions mass transport between the gas and aerosol phases may have to be explicitly modeled. We also predicted that even if the aerosol is in equilibrium with the gas phase, the size distribution of the volatile inorganic components of atmospheric aerosols often cannot be uniquely determined from thermodynamic considerations alone, and thus mass transport usually has to be included to determine the size distribution of the volatile inorganic components (Wexler and Seinfeld, 1990). In a subsequent work, we developed a transport model of atmospheric aerosols that assumes the aerosol particles are in internal equilibrium to predict their surface partial pressures of ammonia and nitric acid, and explicitly models transport between the gas and aerosol phases. In that work we compared the predictions of the model to 1) laboratory measurements and 2) the predictions of other aerosol equilibrium models (Wexler and Seinfeld, 1991). The dynamics of the departure from equilibrium has also been examined by Harrison and MacKenzie (1990), who tested their hypothesis of a kinetically-limited departure from equilibrium with a model of gas-to-particle transport and surface reaction processes.

Comparison of measured gas-phase ammonia and nitric acid concentrations with those predicted from aerosol composition often indicate departures from equilibrium (Cadle *et al.*, 1982; Tanner, 1982; Allen *et al.*, 1989) without identification of the cause for the observed departure. The purpose of the present study is to analyze the ammonium and nitrate size distribution data from the four SCAQS B+ sites (Wall *et al.*, 1988; John *et al.* 1989a, 1989b, 1990), identify departures from equilibrium, and show how these departures correlate to the predicted time constants for equilibration. This work has been reported in full elsewhere (Wexler and Seinfeld, 1992).

A Proposed Indicator for Departure from Equilibrium

Accurate measurement of the aerosol phase ammonium nitrate concentration and the gas-phase ammonia and nitric acid concentrations in the atmosphere are difficult even when sampling times in excess of a few hours are employed. Furthermore a comparison of the measured ammonia, nitric acid, and ammonium concentrations to those predicted by equilibrium calculations often leads to serious disagreement, with the source of

disagreement unidentifiable from the comparison alone. Transport limitations provide one possible explanation for these departures from equilibrium. As we have shown, the time scales for equilibration between the gas and aerosol phases may range from a few seconds to over a day under conditions that often occur in, for instance, the SoCAB (Wexler and Seinfeld, 1990). Thus we seek an indicator of departure from equilibrium, and correlations between this indicator and the estimated time constants for ammonium nitrate equilibration. Observation of such a correlation adds support to the hypothesis that transport limits equilibration between gas and aerosol phase ammonium and nitric acid.

For equilibrium to exist between ammonia and nitric acid in the gas phase, and ammonium nitrate and ammonium sulfate in the aqueous phase, the ratio of aerosol ammonium to aerosol nitrate must be the same for all particle sizes (Wexler and Seinfeld, 1992). Since particles of all sizes are exposed to the same gas phase concentrations of ammonia and nitric acid, the size distribution of ammonium and nitrate must be the same for equilibrium to hold. This suggests an equilibrium indicator based on the overlap between the ammonium and nitrate distributions. We define this overlap C_{an} , which ranges from 1 when the overlap is 100% to zero when there is no overlap for a sample, as

$$C_{an} = 1 - \frac{1}{2} \int_{0.05}^{D_{p,Na}} \left| \frac{M_n(D_p)}{M_n^t} - \frac{M_a(D_p)}{M_a^t} \right| dD_p, \quad (1)$$

where $M_i(D_p)$ and $M_i^t = \int_0^\infty M_i(D_p) dD_p$ are the molar size distribution and total number of moles of nitrate, $i = n$, and ammonium, $i = a$, $D_{p,Na}$ is the size of particle below which the number of moles of sodium is less than one tenth the number of moles of ammonium

$$\int_{0.05}^{D_{p,Na}} M_a(D_p) dD_p > 10 \int_{0.05}^{D_{p,Na}} M_{Na}(D_p) dD_p, \quad (2)$$

where $M_{Na}(D_p)$ is the molar size distribution of sodium.

The time constant, τ_∞ , for equilibration of the gas and aerosol phases is

$$\tau_\infty^{-1} = \frac{3D}{2.303} \int_0^\infty \frac{m(\log_{10} R_p) dR_p}{\left(1 + \frac{\lambda}{\alpha R_p}\right) R_p^3 \rho_p} \quad (3)$$

where $m(\log_{10}(R_p))$ is the aerosol mass distribution, D is the molecular diffusivity, R_p is the particle radius, λ is the mean free path, ρ_p is the particle density, and α is the accommodation coefficient.

Figures 1-3 show the correlation between C_{an} and τ_{∞} , for the summer B+ sites. It is clear from these figures that the aerosol during SCAQS had a wide range of coincidence factors and that the degree of coincidence correlates with the estimated time constant τ_{∞} . The lack of coincidence between the ammonium and nitrate size distributions indicates that the surface partial pressures of ammonia and nitric acid are different for particles of different size, and that these particles are not in equilibrium with each other. Since there is a strong correlation between this lack of equilibrium and the estimated values of τ_{∞} , we can conclude that, as predicted in earlier work, transport limitations contribute to the lack of equilibrium (Wexler and Seinfeld, 1990).

Conclusions

The major hypothesis investigated in this work is that transport on a time scale proportional to τ_{∞} limits equilibration between gas and aerosol phase ammonium nitrate. To investigate the validity of this hypothesis we showed that ammonium nitrate – ammonium sulfate aerosols must have a coincidence factor of unity for all the aerosol particles to be in mutual ammonium nitrate equilibrium, and that lower coincidence factors indicate departures from equilibrium. We demonstrated that a significant correlation existed during SCAQS between the calculated coincidence factors and the estimated time constants. Thus we conclude that transport limitations are a significant factor in the observed departures from equilibrium, but because there is still substantial scatter in the data, we cannot conclude that transport limitations are the sole cause for these observed departures.

Visibility Modeling

Severe visibility reduction is a widely-recognized effect of air pollution in Los Angeles. Work done by Larson *et al.* (1988) has shown that Mie theory calculations can describe local visibility reductions. The measurement programs used to collect data to drive such calculations have generally been both time and work intensive. The question is then raised, can the measurements required to drive a Mie theory scattering calculation be made as part of a continuous air monitoring network. If so, a regional visibility problem could be characterized using a visibility model based on Mie theory calculations, supported by routinely collected data.

The Southern California Air Quality Study, or SCAQS experiments, provide a unique set of data on aerosol size distributions and chemical composition at multiple sites across a large air monitoring network. The SCAQS experiments were carried out in 1987 and over 200 samples are available for visibility modeling. SCAQS sampling sites are

shown in Figure 4, a map of the Los Angeles area. Samples were collected at Claremont, Long Beach, and Rubidoux during five periods in the summer. Central Los Angeles and Long Beach were the site of three winter sampling periods. The information available from the SCAQS experiments includes aerosol size distributions from electrical aerosol analyzers (EAAs), and optical particle counters (OPCs). Filter based chemistry sufficient to estimate the aerosol refractive index is also available as well as nephelometer measurements of light scattering by ambient particles.

Before performing light scattering calculations some basic consistency checks were applied to the data set, including aerosol anion and cation balances, material balances on the chemical composition of filter samples, and a comparison of aerosol volume from the size distributions to the volume inferred from the filter samples. Comparisons were also made of scattering coefficients measured with nephelometers at the same site. Figure 5 illustrates the anion-cation balance for Long Beach in August and September for the PM10 sample. Each paired set of stacked bar graphs shows the anion and cation concentrations for a sampling period. There is a good cation-anion balance for these samples as is true for the data set in general.

Figures 6, 7, and 8 show comparisons of the gravimetrically determined filter mass and the sum of the mass of the chemically species. These figures show that there is a good material balance for Claremont in the summer and Long Beach and Central Los Angeles in the fall. Figures 9, 10 and 11 are comparisons of the volumes. Comparisons are made between the volume measured with the EAA and OPC and the volume inferred from the filter measurements. These figures show that the two measurements are highly correlated, although there is not a one-to-one correlation in all instances. At some sites more than one nephelometer was used to make measurement of the light scattering coefficient. Data is available from three instruments at Claremont. There are differences between the instruments in their wavelength sensitivities and the presence or absence of heated inlets. One would expect the relationship or ordering of the data from the different instruments to remain relatively constant. This is generally the case at Claremont, although not at Long Beach. No visibility could be expected to agree with all the nephelometer measurements given the disagreement seen in the measured values in Figures 12 and 13. To perform a Mie theory calculation of the light scattering coefficient it is necessary to know the aerosol size distribution and the refractive index of the aerosol. The refractive index was calculated from the filter based chemistry with two approaches, as a volume average and using partial MOLAR refractive indices. Both methods provide nearly identical values. It is noted that the light scattering coefficient calculated by Mie theory is more sensitive to variations of the aerosol size distribution than variations in the refractive index.

Aerosol size distribution information is available from three instruments, with data for over 100 channels with some overlap. Figure 14 shows the raw size distribution data for the sampling period beginning at midnight in Claremont on the 27th of August. The EAA is shown with a solid line and the two OPCs are shown with broken lines. Figure 15 shows similar data for the sampling period beginning at 9:00 a.m. in Claremont on the 27th of August. We see similar patterns of overlap and agreement between the instruments in these figures. For a final size distribution used in calculations, no overlap is desired, and the data is taken from the most reliable channels of the instrument. In Figure 16 we see a final aerosol size distribution for all sampling periods of August 27 at Claremont. Data is taken from the EAA for diameters less than .23 micron and the PMS/OPC data is used between .23 and 2.5 microns. Comparisons of the gravimetrically inferred volume between 2.5 and 10 microns suggest that the Climet OPC underestimates the volume present in this size range. Figure 16 also illustrates a uniform $dV/d\log D_p$ distribution used between 2.5 and 10 microns with a volume matching that inferred from the filter samples.

To carry out the actual Mie scattering calculation a scattering efficiency is calculated for each diameter. The particle light scattering coefficient is then the integral over the size distribution of the product of scattering efficiency and the number of particles. Light scattering coefficients were calculated with three different cases of aerosol size distributions. In case A, only fine particle data for diameters less than 2.5 micron was used. In case B, a uniform $dV/d\log D_p$ distribution was included for the coarse aerosol, and in case C the size distribution from the EAA and OPC was rescaled to match the aerosol volume inferred from the filter samples. Figure 17 shows a comparison between the observed light scattering coefficients and those calculated with our model. Observations are shown with a solid line and the model results are shown with a dash line. This time series is for size distribution case A in Claremont in the summer sample periods. There is relatively good agreement between observations and the model result at this site with some underprediction in September. The model results shown in Figure 18 are virtually the same when aerosol size distribution case B is used. The inclusion of the coarse aerosols does not affect the results markedly. This is not surprising as particles in the 0.1 to 1 micron diameter range dominate light scattering. Figure 19 illustrates the results for Claremont using aerosol size distribution case C. We see some improvement in agreement, particularly in June and September, and some overestimation in July and August for Claremont. Figure 20 shows the results for Long Beach in the summer. We see underprediction in all cases using aerosol size distribution case A. In Figure 21, using aerosol size distribution case C, the results are improved and agreement is good in June and July and improvement is seen for August and September. Figure 22 shows a time

series of the results for Central Los Angeles. We see relatively good agreement between model predictions and observations in November and overprediction by the model in December. Using aerosol size distribution case C, when the volume is rescaled to match the volume inferred from the filter we see improvement in the December results in Central Los Angeles. Regression analysis shows relatively high correlation coefficient for Claremont and the underprediction at Long Beach in the summer is reflected in the low value of alpha (Tables 1 and 2). The overprediction at Central Los Angeles is likewise reflected in the high value of alpha. The regression results for aerosol size distribution case C show higher correlation coefficients in all cases and values of alpha closer to unity.

Conclusions

The conclusions we can draw from this work are that the SCAQS network aerosol data can be used to support visibility model calculations. There is a good fine particle ion balance and a reasonable fine particle material balance. The fine aerosol volume from the EAA and the OPC data are highly correlated with the volume inferred from fine filter samples. It is also noted that co-located nephelometers are often in disagreement. Therefore, no light scattering model can agree with all of the nephelometer data. The light scattering values calculated assuming dry aerosol match nephelometer light scattering measurements well in those cases where the nephelometer data are not in doubt. It appears possible to maintain a network of monitoring sites that can be used to track the effective pollutant properties on visibility using Mie theory calculations.

References

- Allen, A.G., R. M. Harrison and J. Erisman (1989) "Field measurements of the dissociation of ammonium nitrate and ammonium chloride aerosols," *Atmos. Environ.*, **23**, 1591-1599.
- Bassett, M., and J. H. Seinfeld (1983) "Atmospheric equilibrium model of sulfate and nitrate aerosols," *Atmos. Environ.*, **17**, 2237-2252.
- Bassett, M. E., and J. H. Seinfeld (1984) "Atmospheric equilibrium model of sulfate and nitrate aerosols – II. Particle size analysis," *Atmos. Environ.*, **18**, 1163-1170.
- Cadle, S.H., R. J. Countess and N. A. Kelley (1982) "Nitric acid and ammonia in urban and rural locations," *Atmos. Environ.*, **16**, 2501-2506.
- Doyle, G.J., E. C. Tuazon, R. A. Graham, T. M. Mischke, A. M. Winer and J. N. Pitts (1979) "Simultaneous concentrations of ammonia and nitric acid in a polluted atmosphere and their equilibrium relationship to particulate ammonium nitrate," *Environ. Sci. Technol.*, **13**, 1416-1419.
- Grosjean, D. (1982) "The stability of particulate nitrate in the Los Angeles atmosphere," *Sci. Total Environ.*, **25**, 263-275.

- Harrison, R.M. and A. R. MacKenzie (1990) "A numerical simulation of kinetic constraints upon achievement of the ammonium nitrate dissociation equilibrium in the troposphere," *Atmos. Environ.*, **24A**, 91-102.
- Hildemann, L. M., A. G. Russell and G. R. Cass (1984) "Ammonia and nitric acid concentrations in equilibrium with atmospheric aerosols: experiment vs theory," *Atmos. Environ.*, **18**, 1737-1750.
- John, W., S. M. Wall, J. L. Ondo and W. Winklmayr (1989a) "Acidic size distributions during SCAQS," *California Air Resources Board*, **A6-112-32**.
- John, W., S. M. Wall, J. L. Ondo, and W. Winklmayr (1989b) "Acidic aerosol size distributions during SCAQS. Compilation of data tables and graphs," *California Air Resources Board*, **A6-112-32**.
- John W., S. M. Wall, J. L. Ondo and W. Winklmayr (1990) "Modes in the size distributions of atmospheric inorganic aerosol," *Atmos. Environ.*, **24A**, 2349-2359.
- Larson, S.M., K. J. Hussey, F. Luce and Glen R. Cass (1988) "Verification of Image Processing-Based Visibility Events in the Los Angeles Area," *Env. Sci. and Tech.*, **22**, 629-637.
- Pilinis, C. and J. H. Seinfeld (1987) "Continued development of a general equilibrium model for inorganic multicomponent atmospheric aerosols," *Atmos. Environ.* **21**, 2453-2466.
- Pilinis, C. and J. H. Seinfeld and C. Seigneur (1987) "Mathematical modeling of the dynamics of multicomponent atmospheric aerosols," *Atmos. Environ.*, **21**, 943-955.
- Pilinis C. and J. H. Seinfeld (1988) "Development and evaluation of an Eulerian photochemical gas-aerosol model," *Atmos. Environ.*, **22**, 1985-2001.
- Russell A. G., G. J. McRae and G. R. Cass (1983) "Mathematical modeling of the formation and transport of ammonium nitrate aerosol," *Atmos. Environ.* **17**, 949-964.
- Russell, A. G. and G. R. Cass (1986) "Verification of a mathematical model for aerosol nitrate and nitric acid formation and its use for control measure evaluation," *Atmos. Environ.*, **20**, 2011-2025.
- Russell, A.G., McCue, K. F. and G. R. Cass (1988) "Mathematical modeling of the formation of nitrogen-containing air pollutants. 1. Evaluation of an Eulerian photochemical model," *Environ. Sci. Technol.*, **22**, 263-271.
- Saxena, P., C. Seigneur and T. W. Peterson (1983) "Modeling of multiphase atmospheric aerosols," *Atmos. Environ.*, **17**, 1315-1329.
- Saxena, P., A. B. Hudischewskyj, C. Seigneur and J. H. Seinfeld (1986) "A comparative study of equilibrium approaches to the chemical characterization of secondary aerosols," *Atmos. Environ.*, **20**, 1471-1483.
- Stelson, A.W., S. K. Friedlander and J. H. Seinfeld (1979) "A note on the equilibrium relationship between ammonia and nitric acid and particulate ammonium nitrate," *Atmos. Environ.*, **13**, 369-371.

- Tanner, R. L. (1982) "An ambient experimental study of phase equilibrium in the atmospheric system: aerosol H^+ , NH_4^+ , SO_4^{2-} , $NO_3^- - NH_3(g)$, $HNO_3(g)$," *Atmos. Environ.*, **16**, 2935-2942.
- Wall, S.M., W. John and J. L. Ondo (1988) "Measurement of aerosol size distributions for nitrate and major ionic species," *Atmos. Environ.*, **22**, 1649-1656.
- Wexler, A. S. and J. H. Seinfeld (1990) "The distribution of ammonium salts among a size and composition dispersed aerosol," *Atmos. Environ.* **24A**, 1231-1246.
- Wexler, A. S. and J. H. Seinfeld (1991) "Second-generation inorganic aerosol model," *Atmos. Environ.* **25A**, 2731-2748.
- Wexler, A. S. and J. H. Seinfeld (1992) "Analysis of aerosol ammonium nitrate: Departures from equilibrium during SCAQS," *Atmos. Environ.*, **26A**, 579-591.

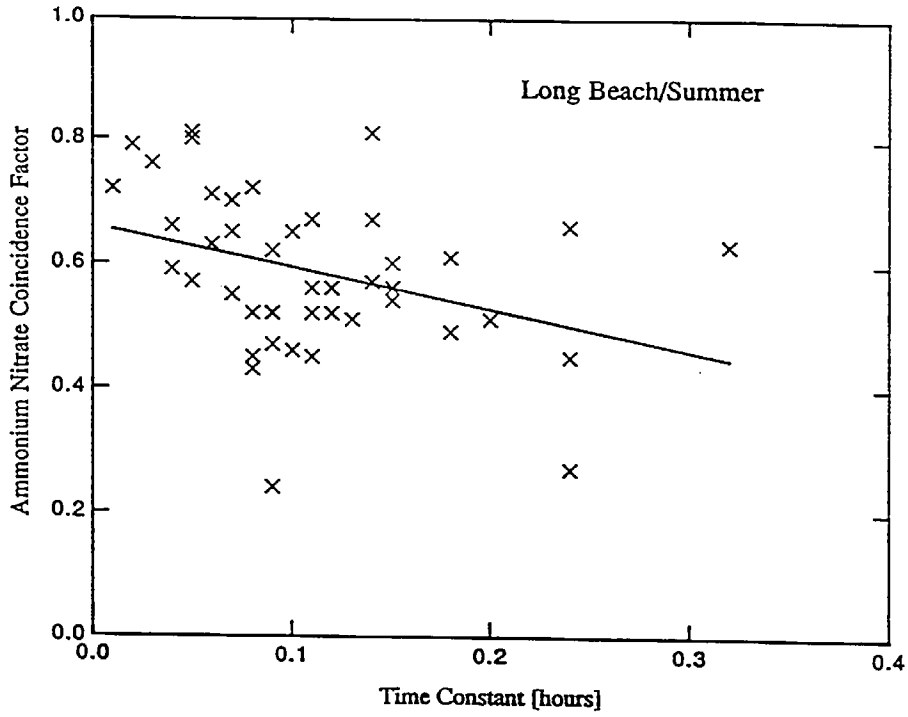
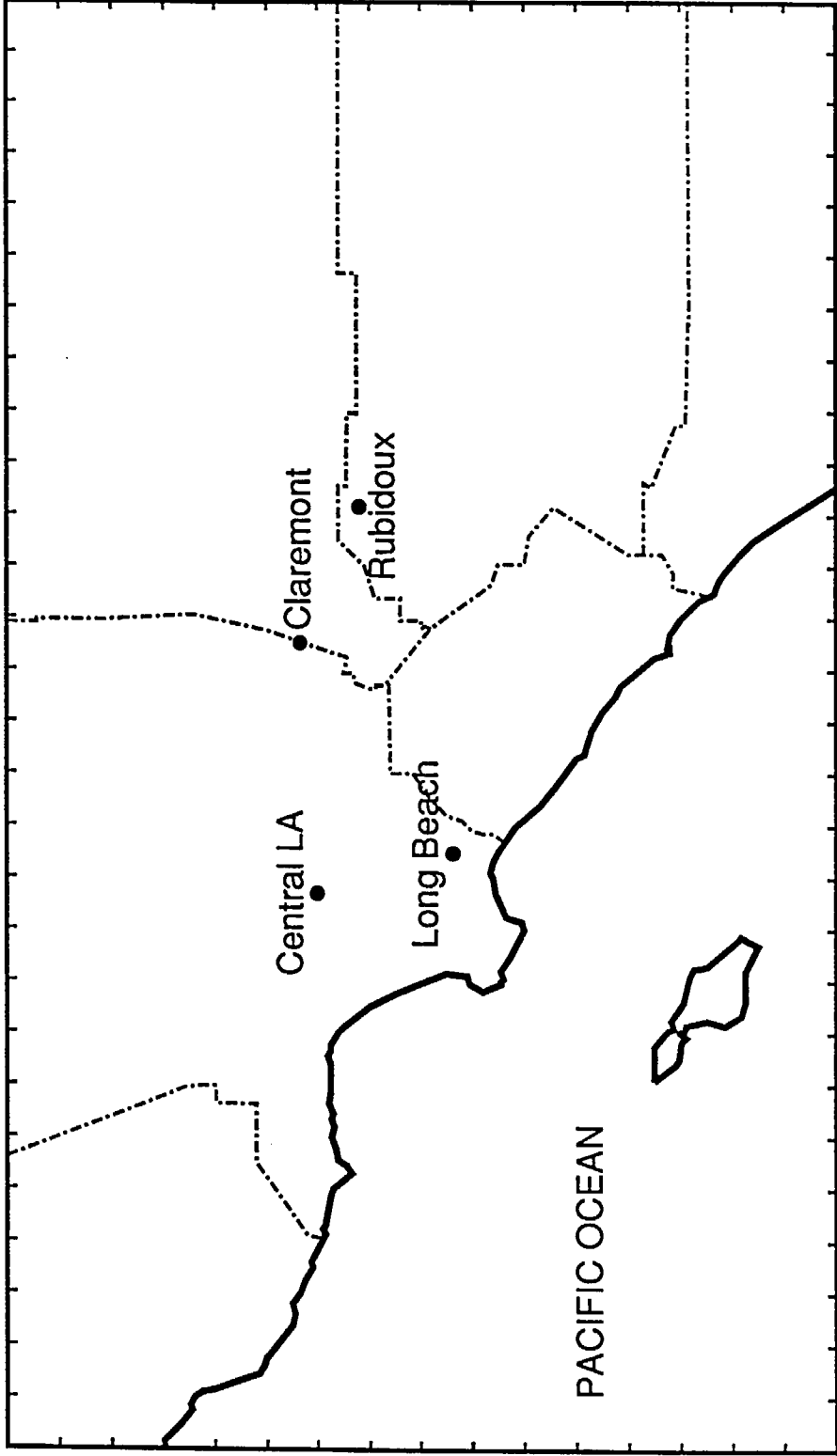


Figure 3: The ammonium nitrate coincidence factor as a function of the equilibration time scale τ_{∞} for Long Beach, CA in the summer.



SCAQS sampling sites

Figure 4

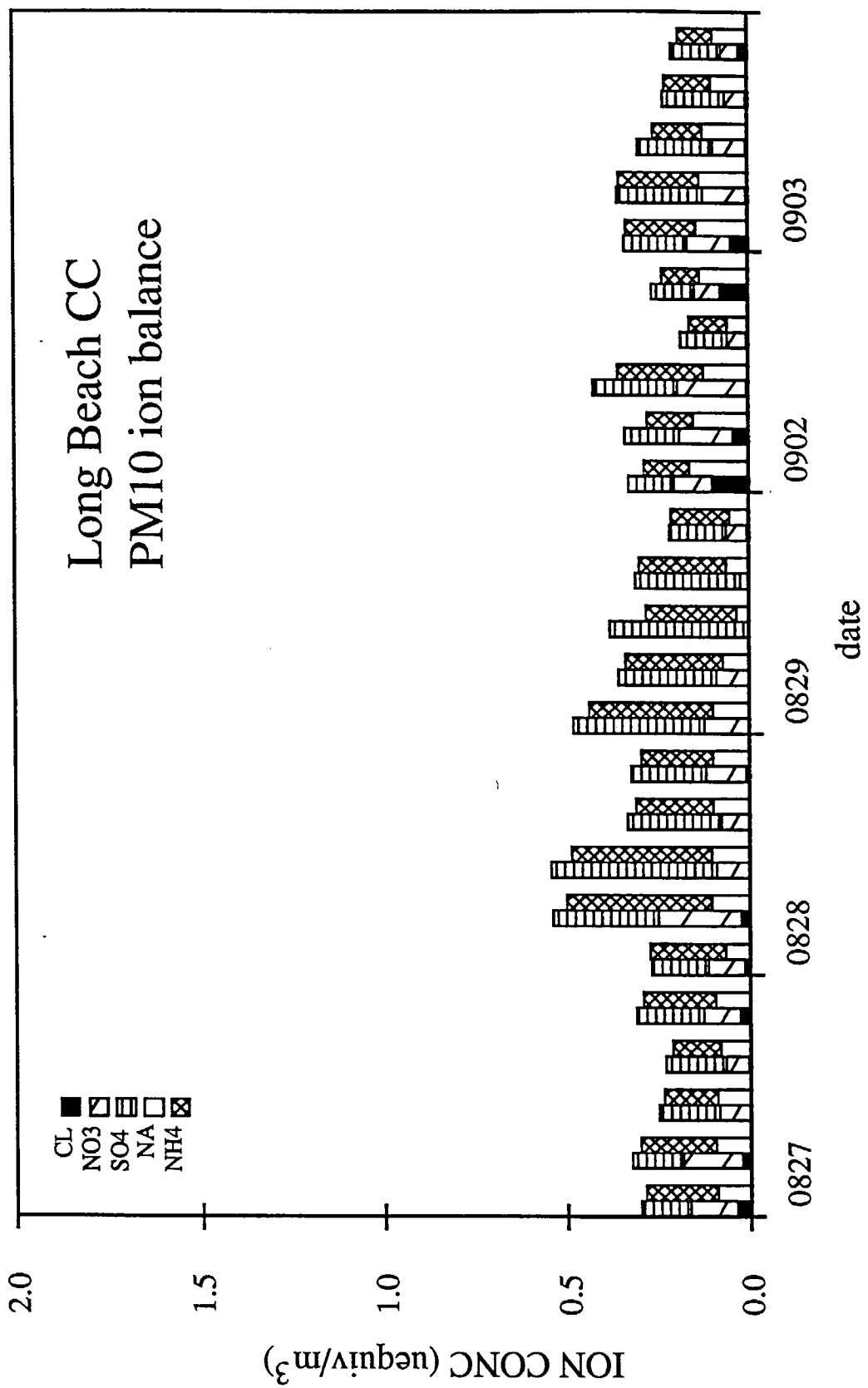


Figure 5

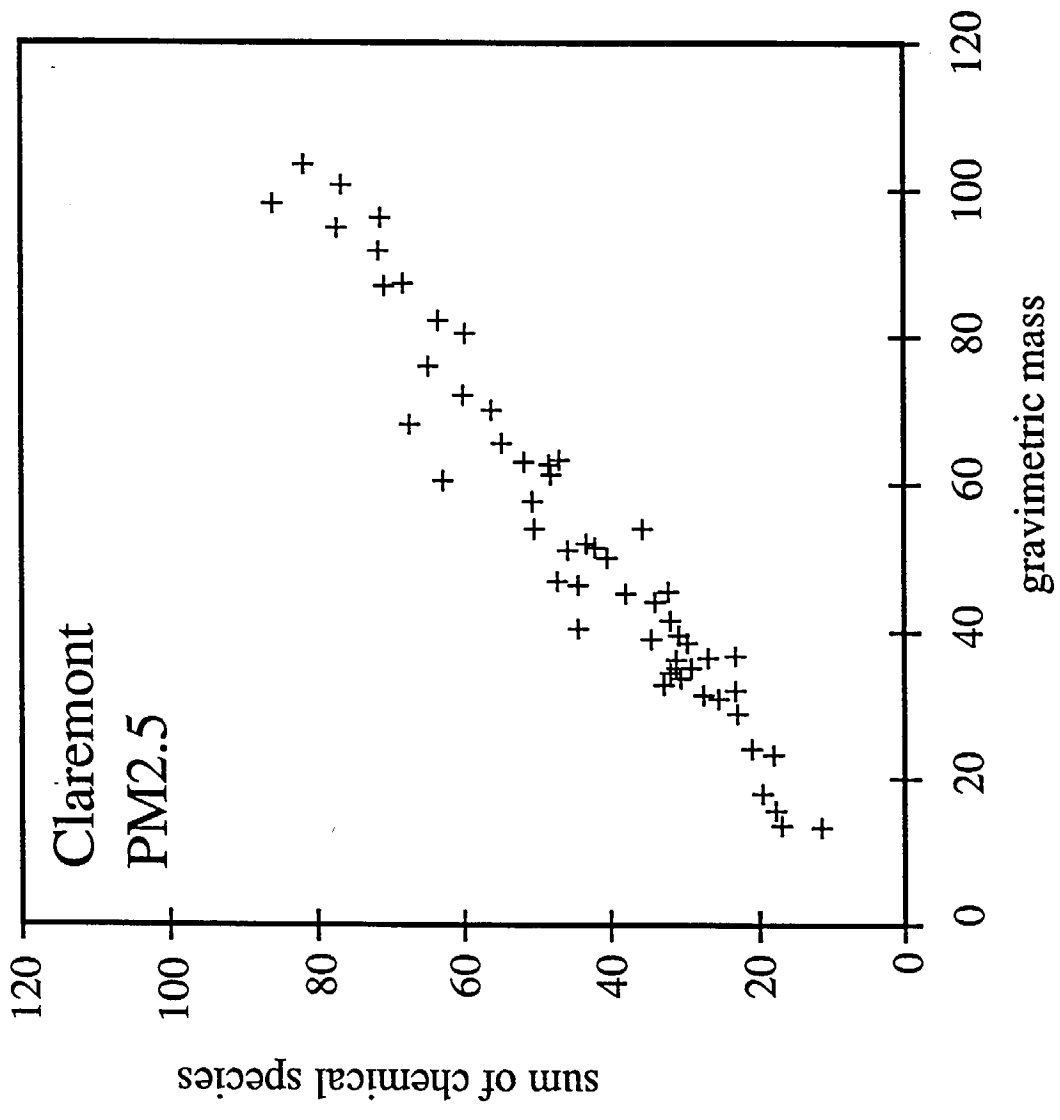


Figure 6

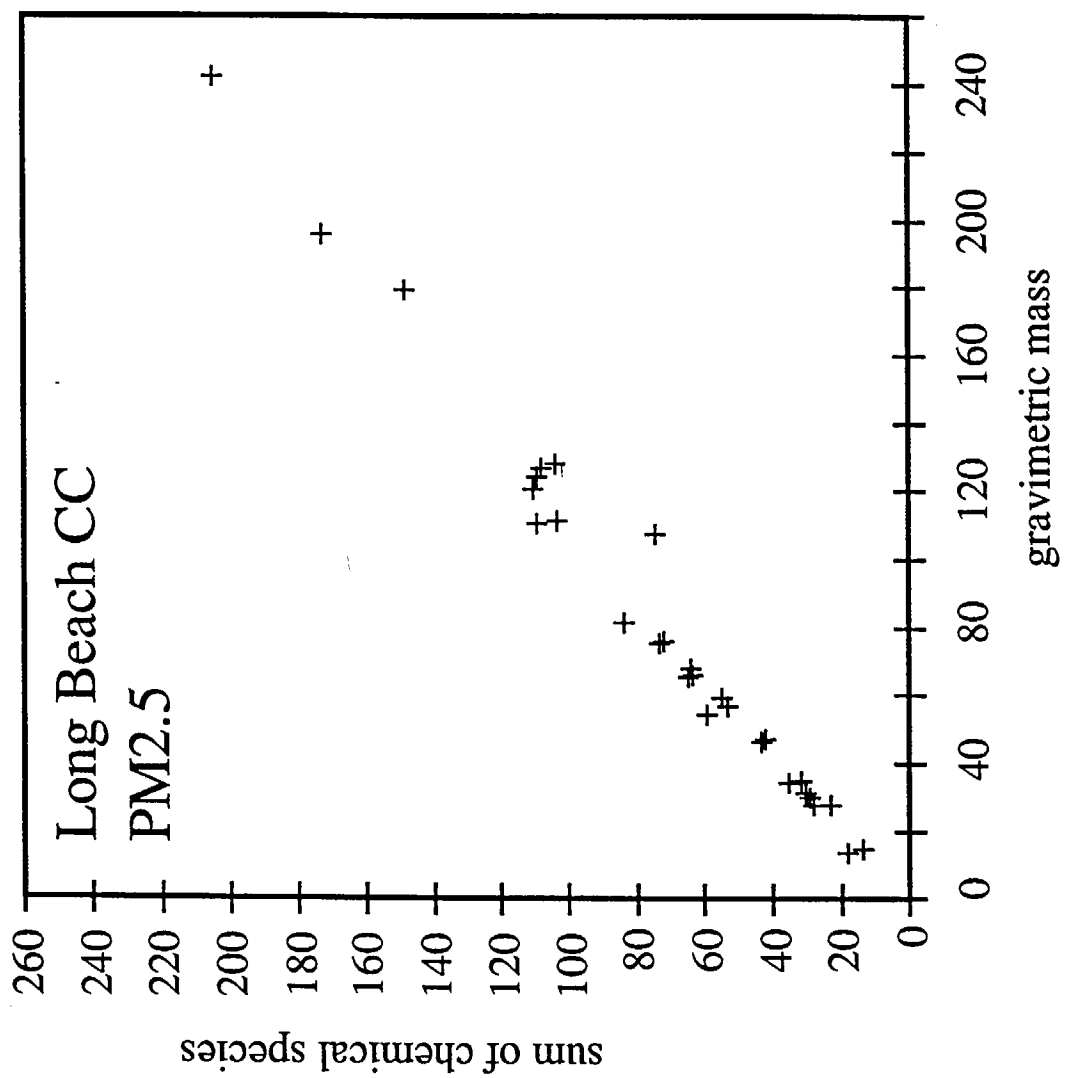


Figure 7

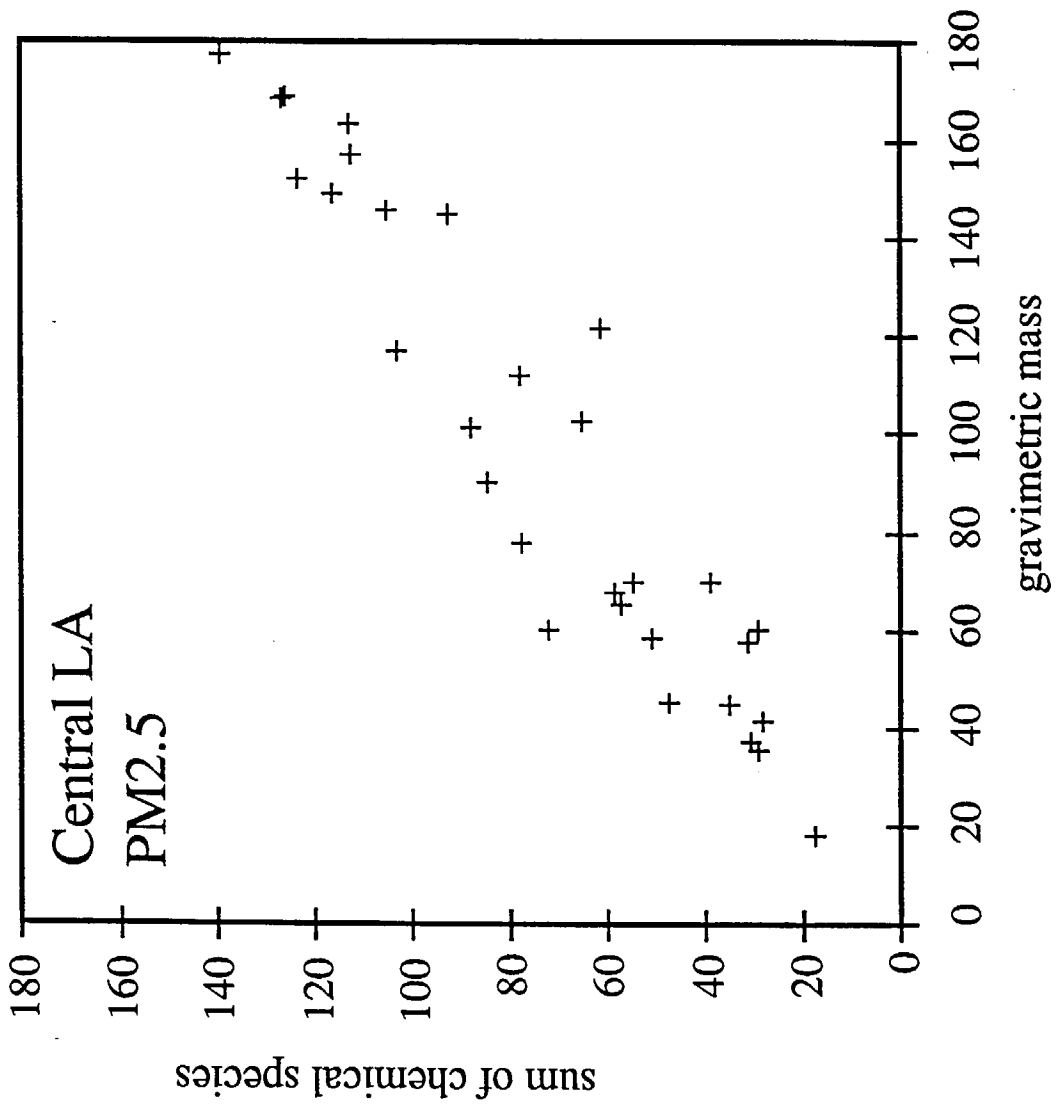


Figure 8

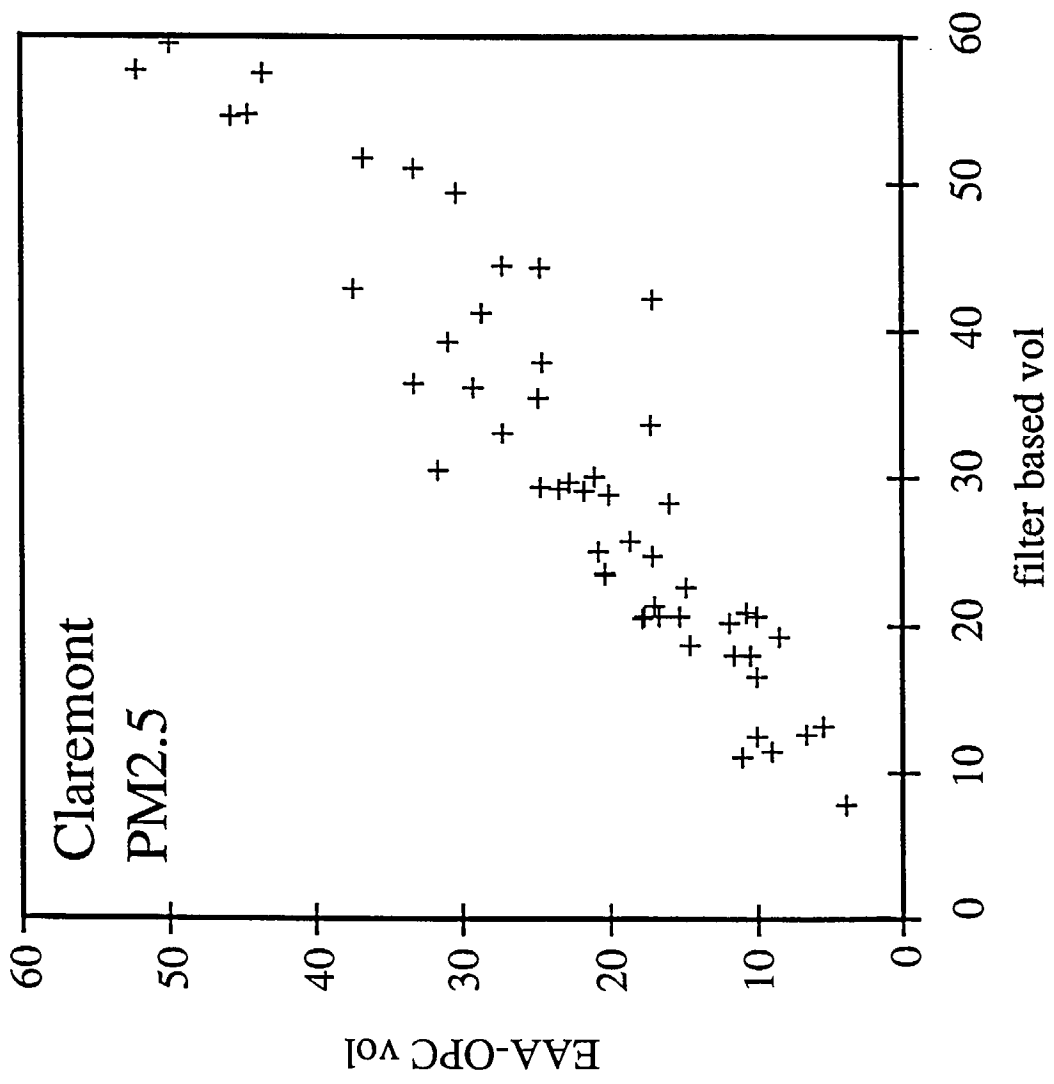


Figure 9

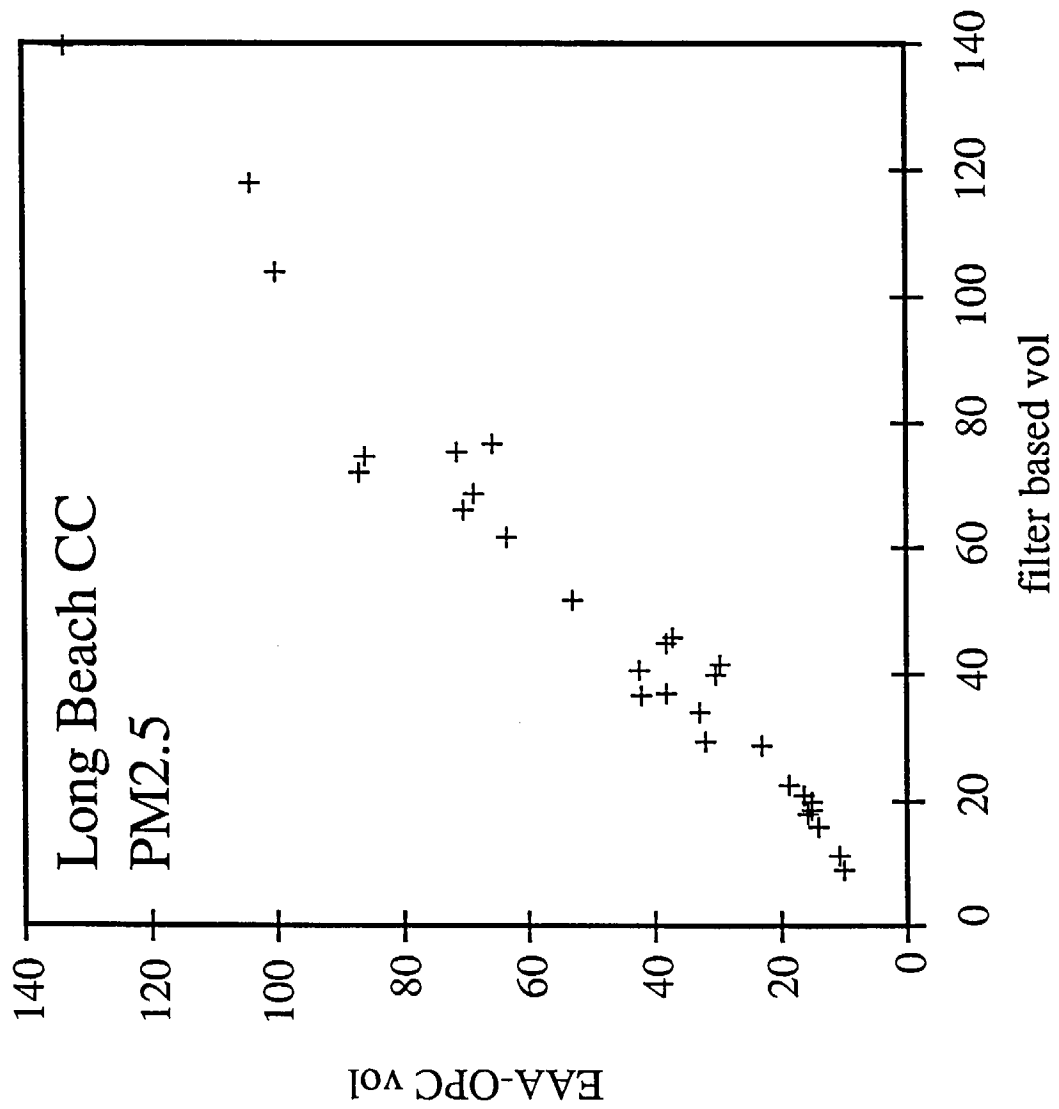


Figure 10

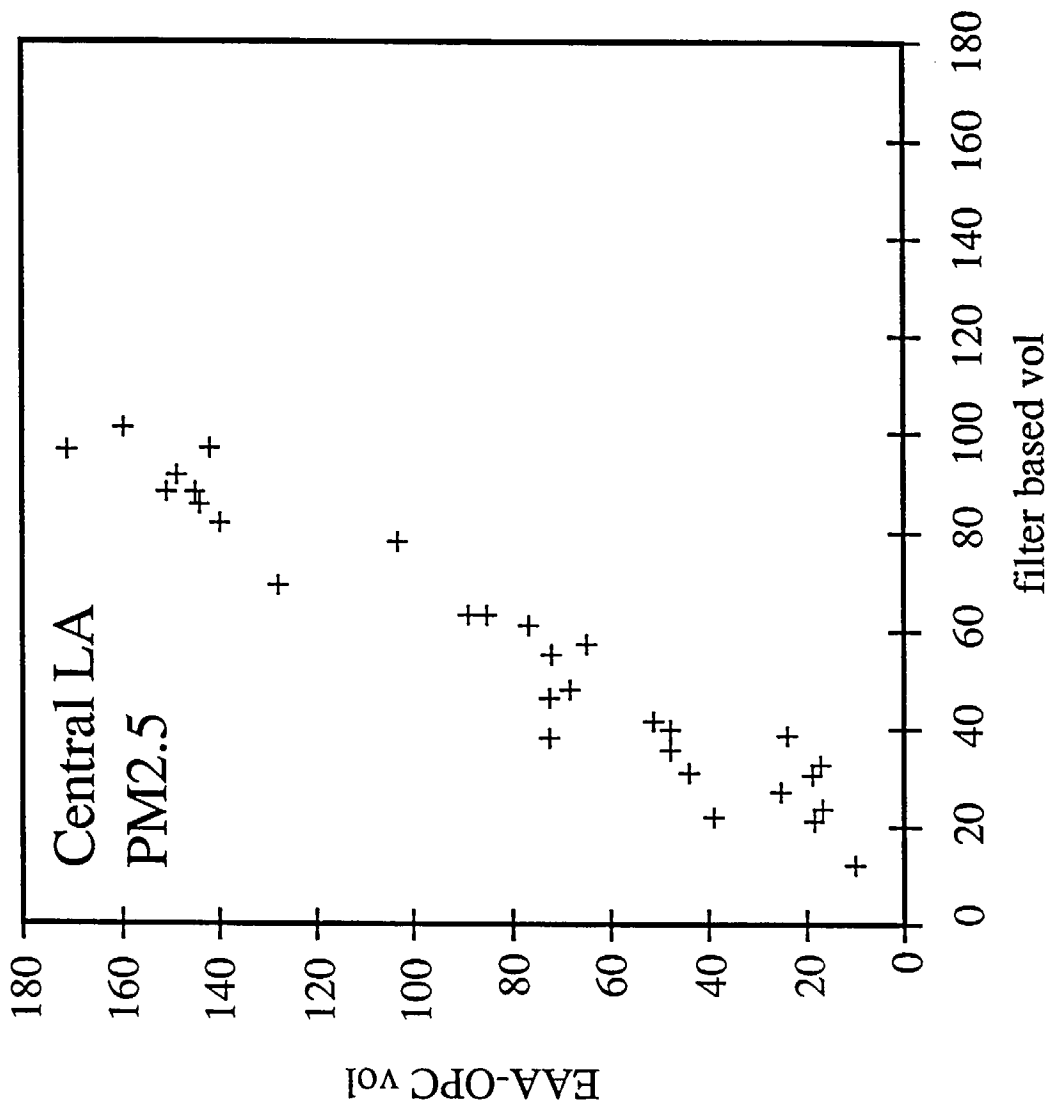


Figure 11

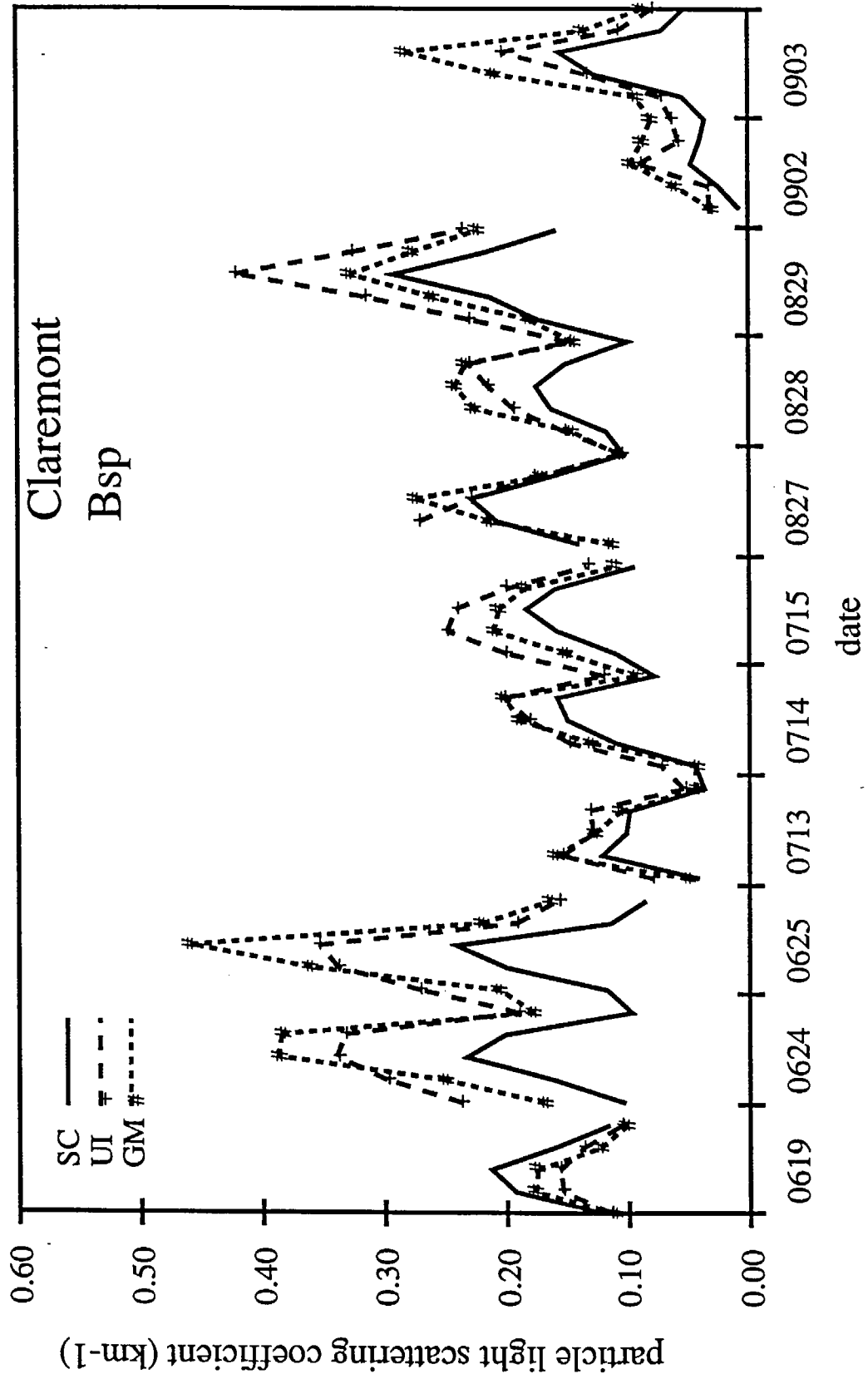


Figure 12

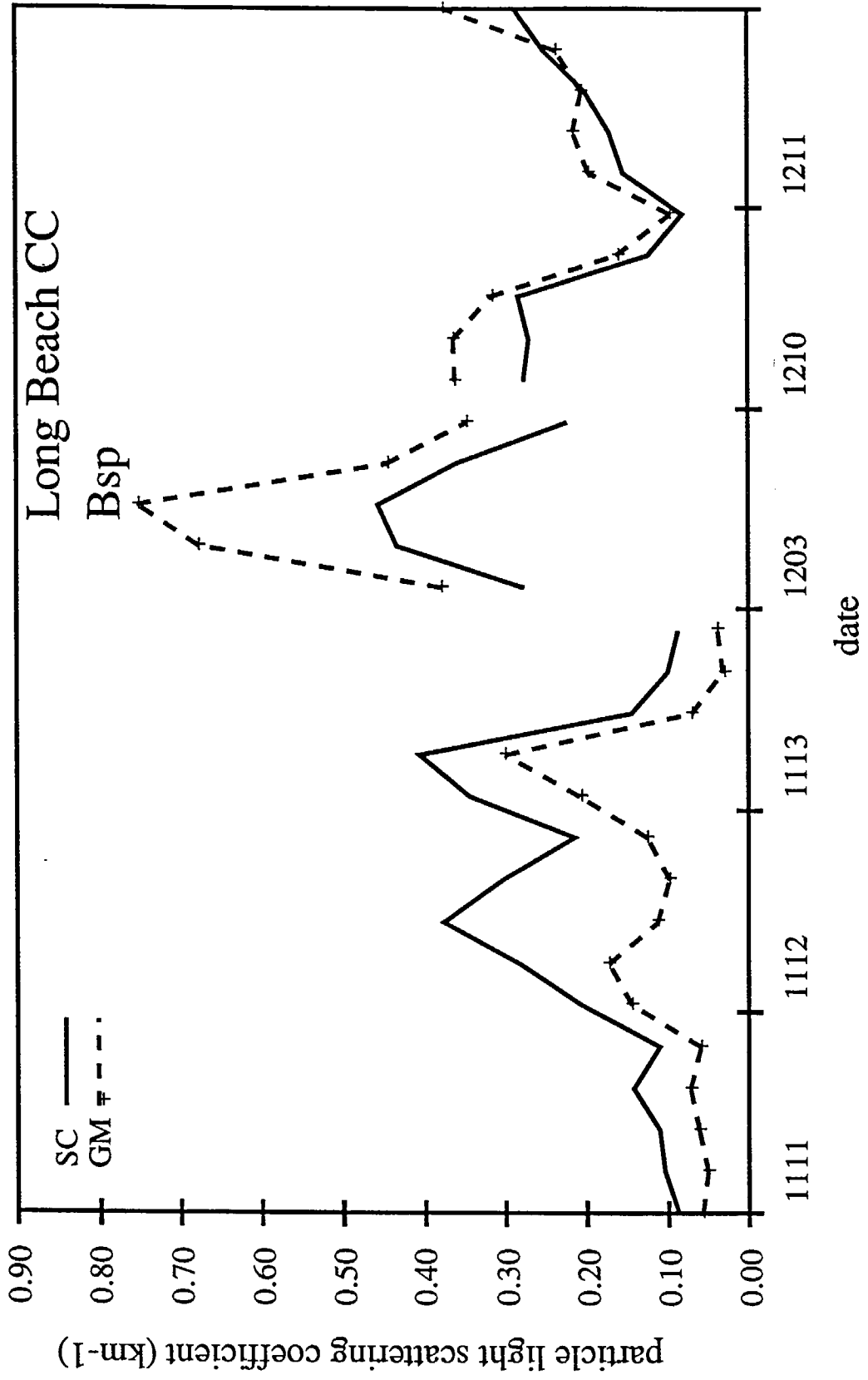


Figure 13

raw aerosol size distribution information

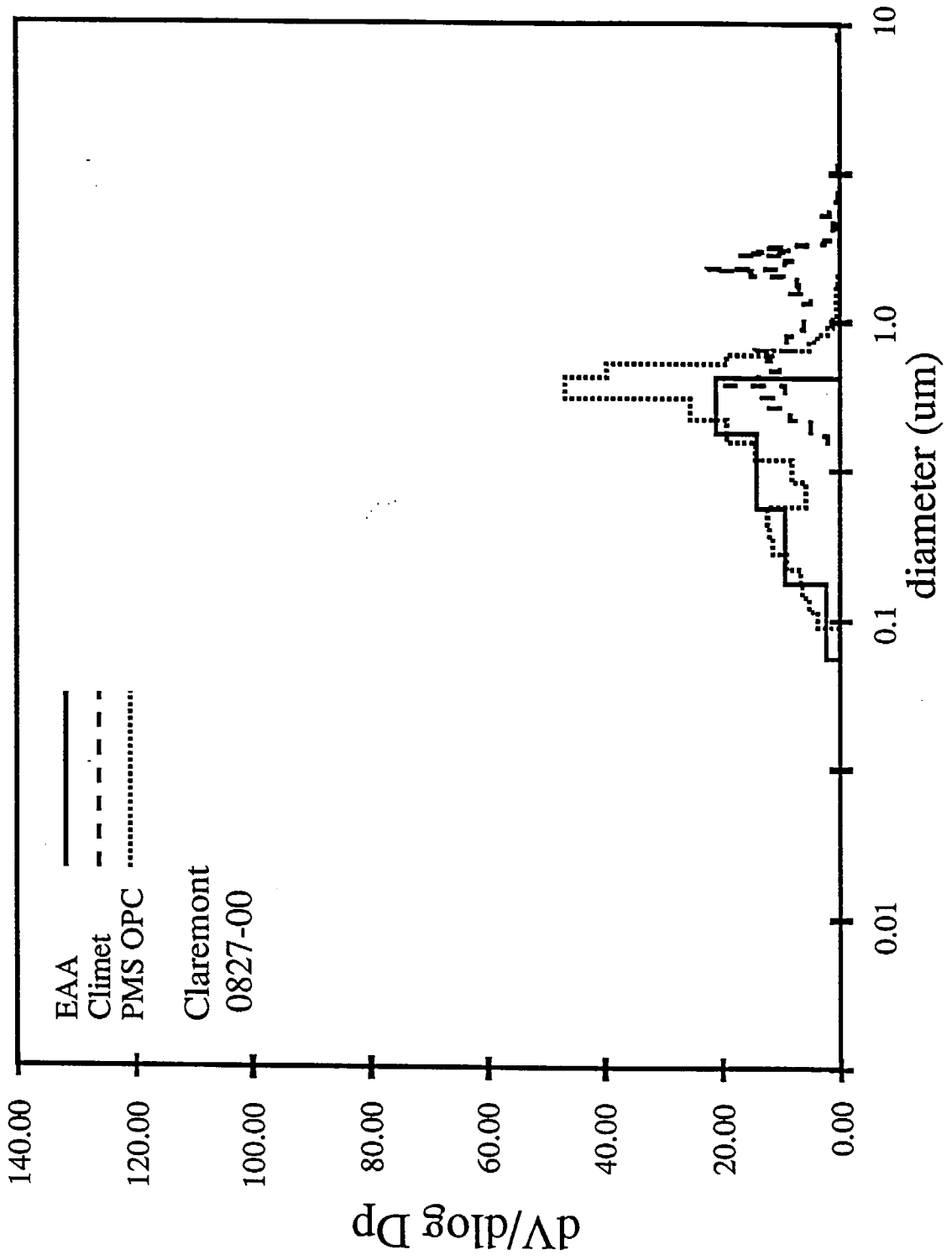


Figure 14

raw aerosol size distribution information

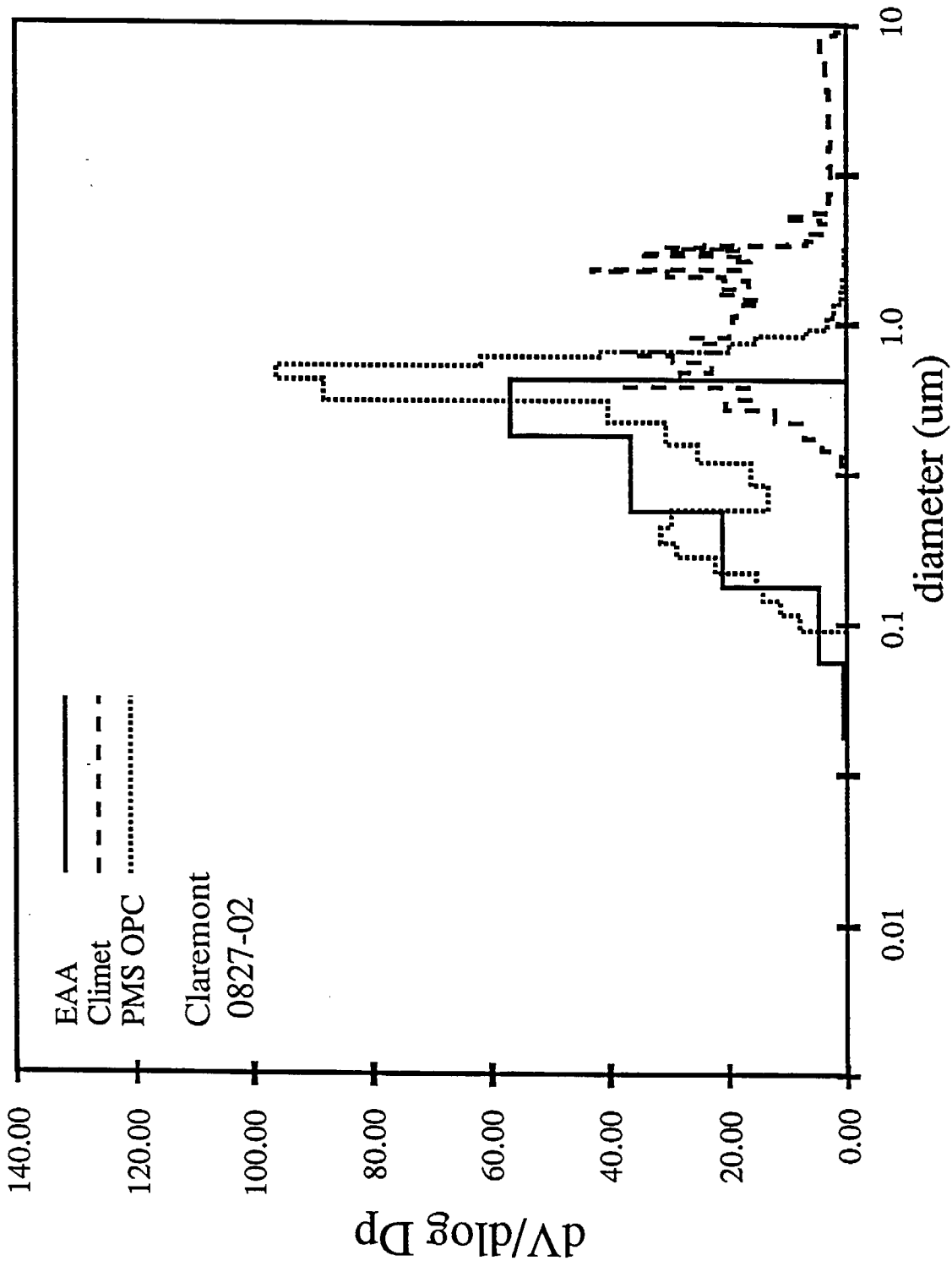


Figure 15

final size distribution used in calculations

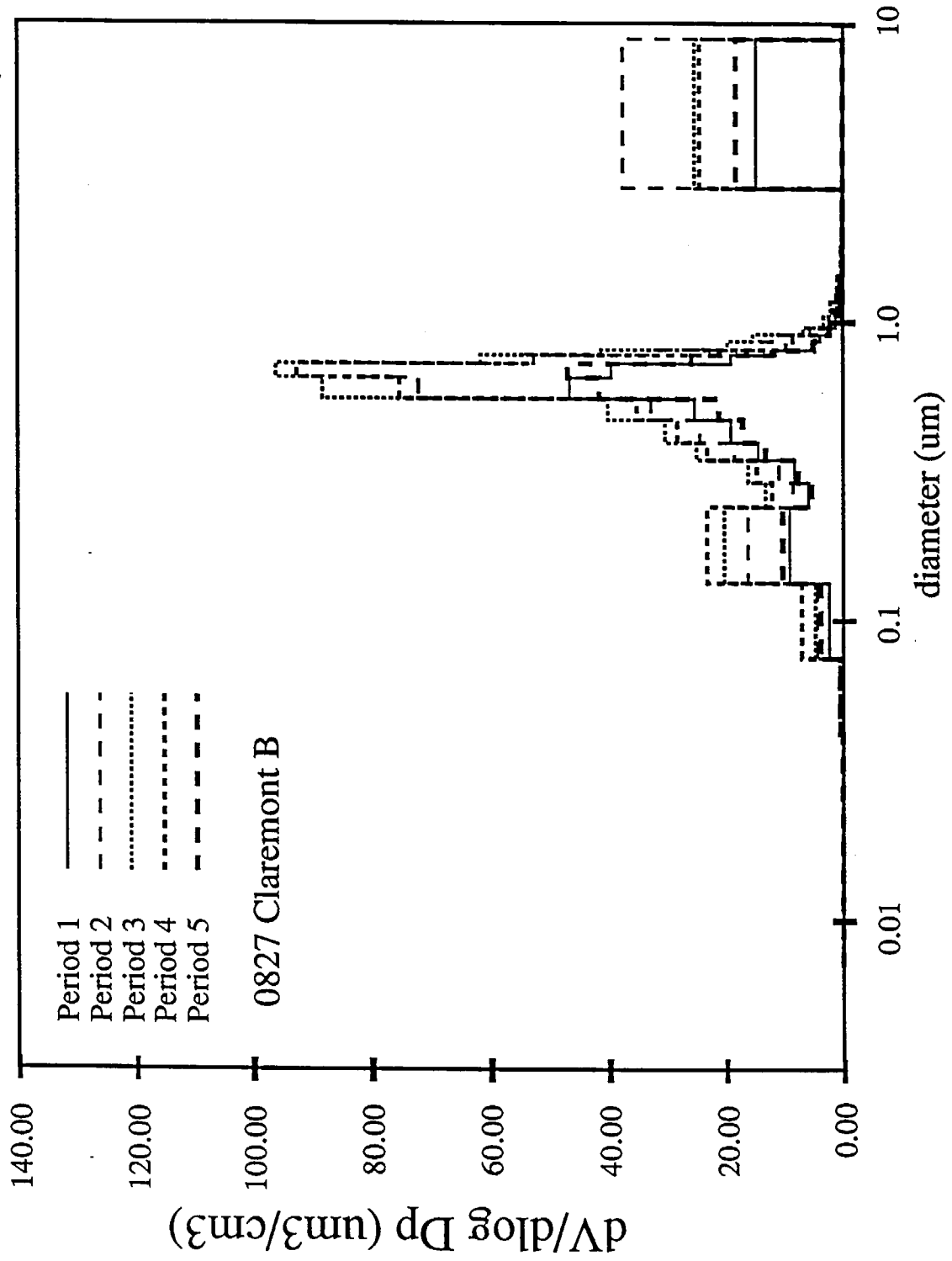


Figure 16

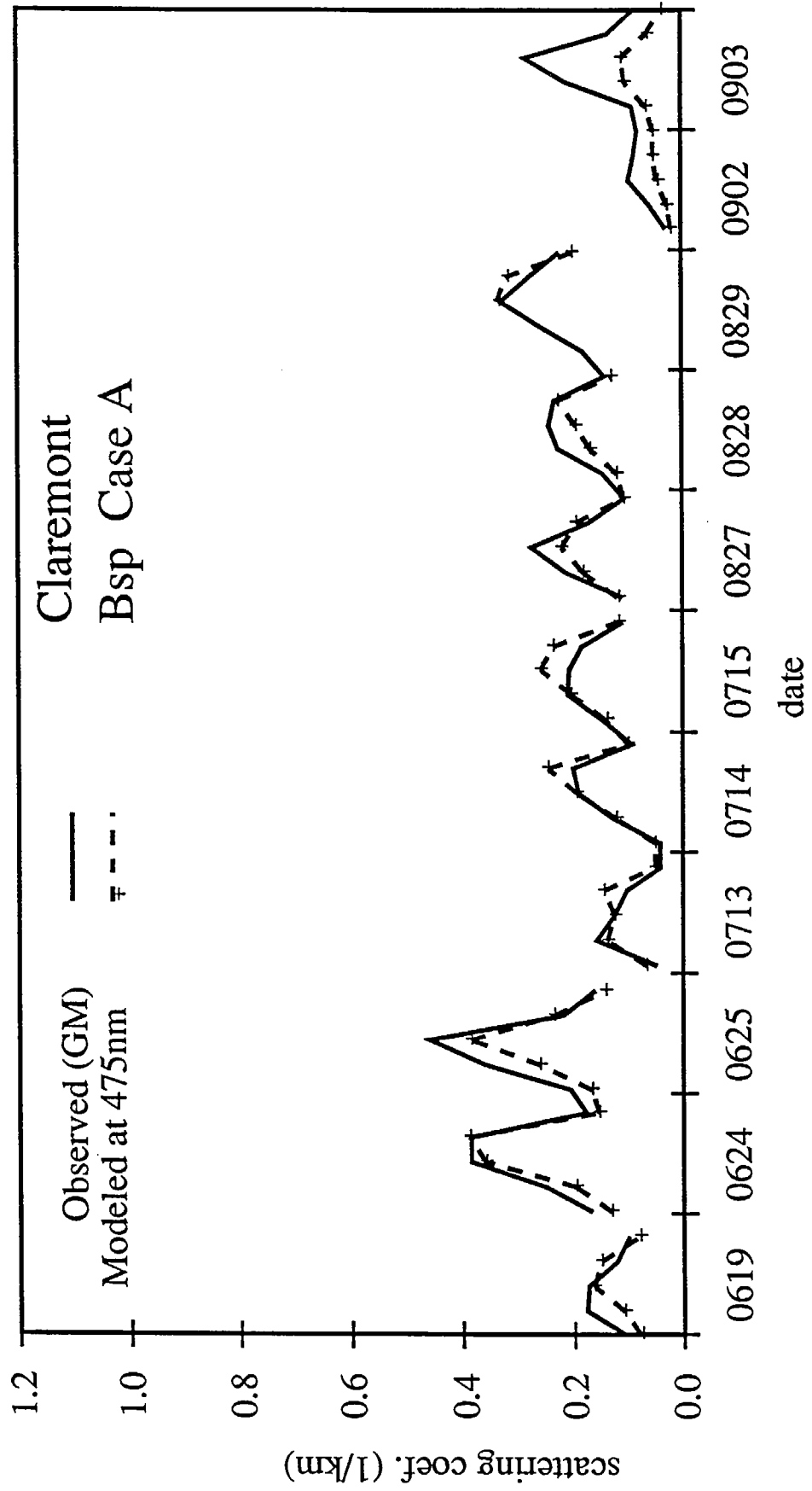


Figure 17

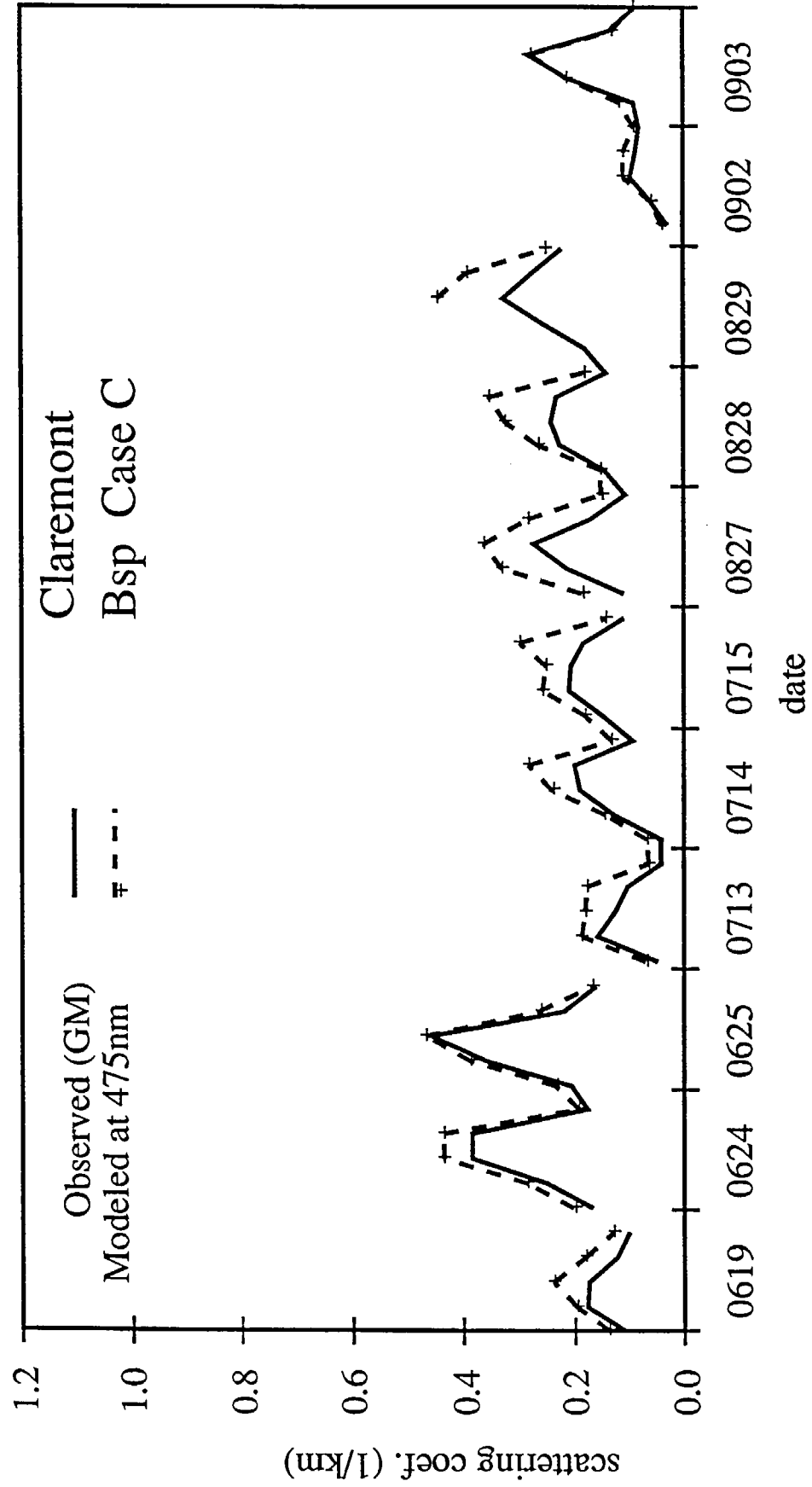


Figure 19

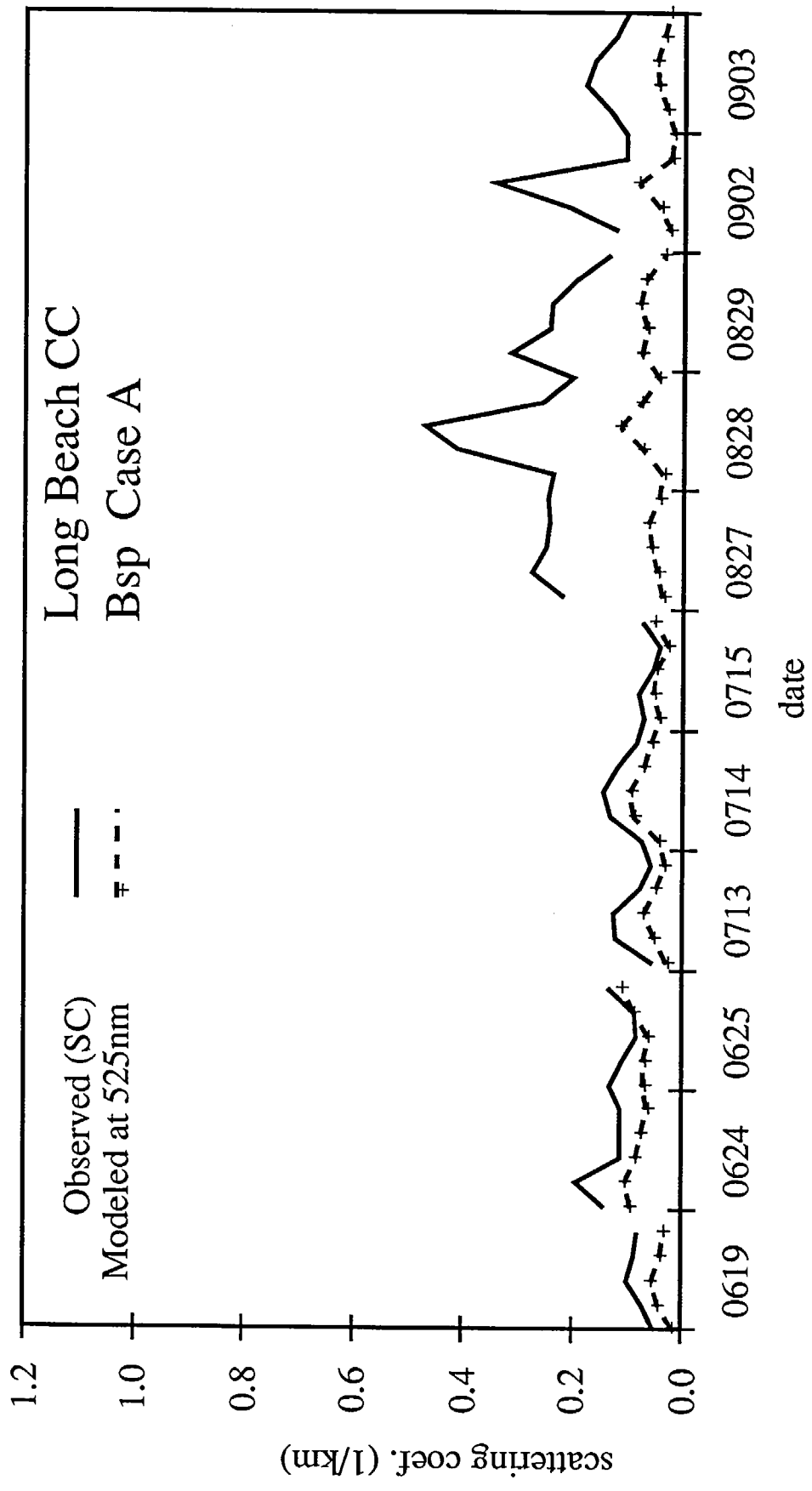


Figure 20

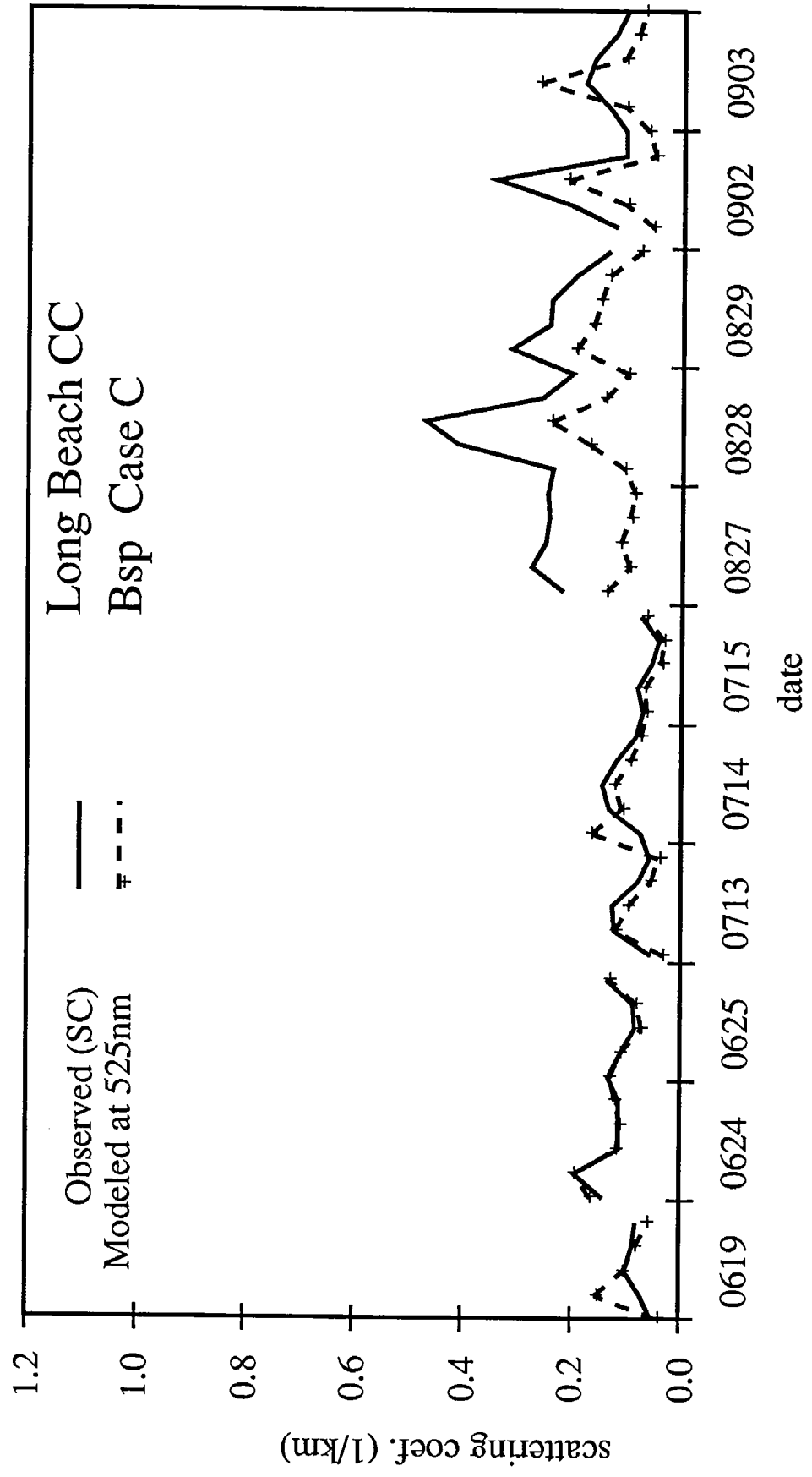


Figure 21

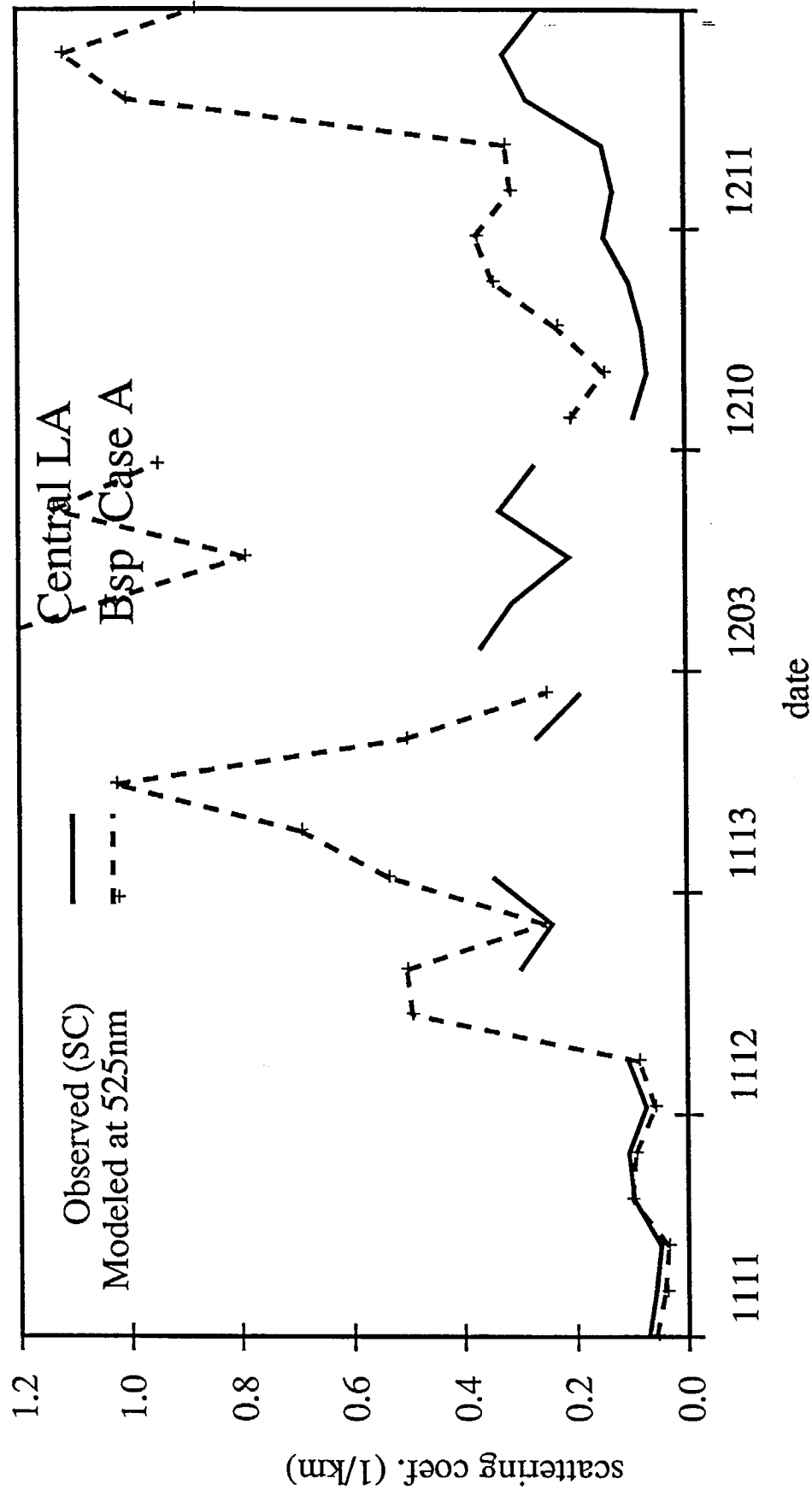


Figure 22-A

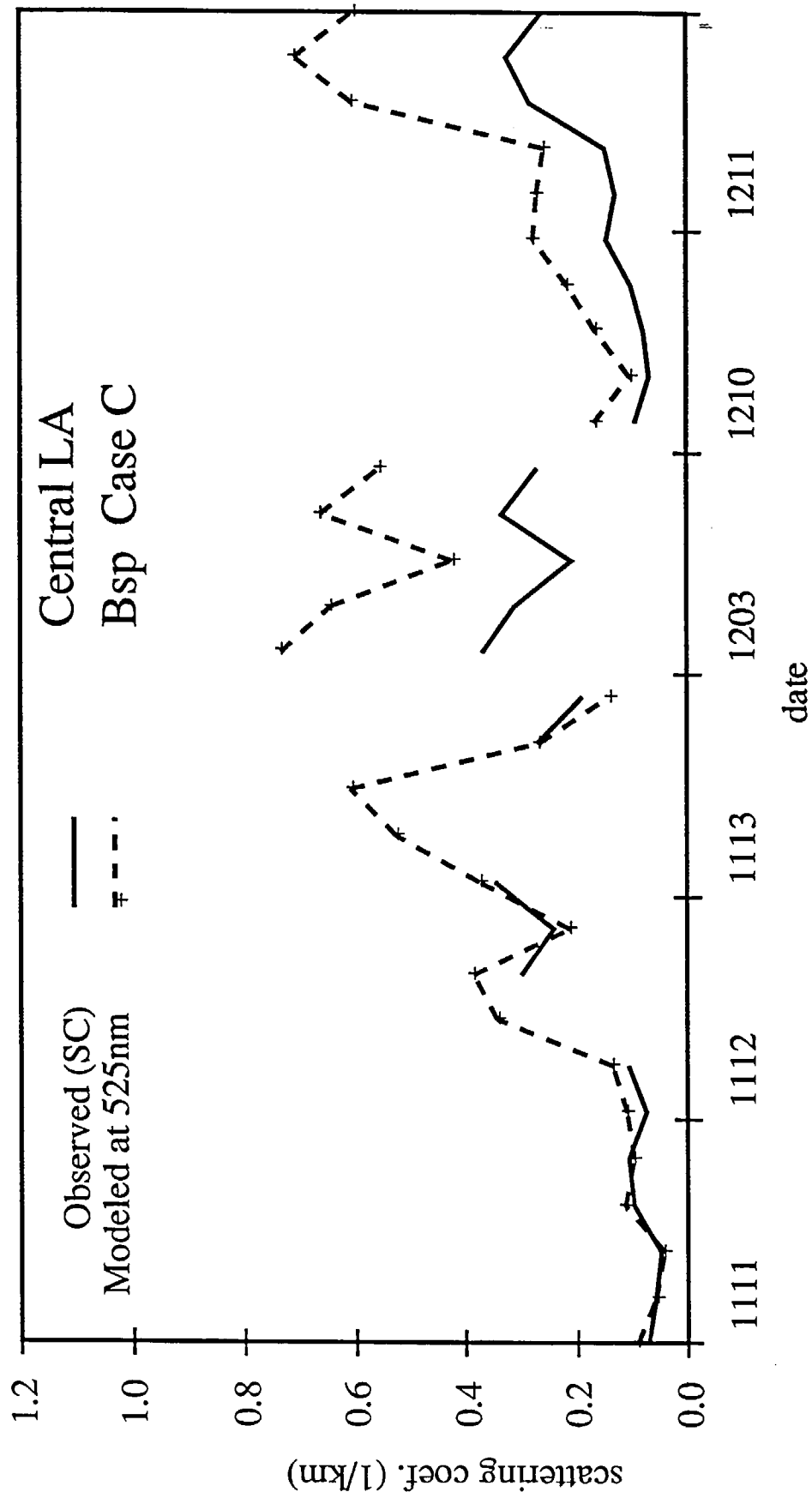


Figure 22-B

Regression Analysis - Case A

$$\text{Predicted} = \alpha \text{ Observed} + \beta$$

alpha	beta	n	(r)
Case A			
	Claremont GM		summer
0.874	0.030	53	0.900
	Long Beach CC SC		summer
0.120	0.058	55	0.457
	Long Beach CC GM		fall
1.352	0.043	29	0.957
	Central LA SC		fall
3.340	-0.135	27	0.873

Table 1

Regression Analysis - Case C

$$\text{Predicted} = \alpha \text{ Observed} + \beta$$

alpha	beta	n	(r)
Case C			
	Claremont GM		summer
1.113	0.050	53	0.952
	Long Beach CC SC		summer
0.379	0.069	55	0.681
	Long Beach CC GM		fall
1.400	0.047	29	0.964
	Central LA SC		fall
1.873	-0.019	27	0.879

Table 2

Disclaimer

The statements and conclusions in this report are those of the contractor and not necessarily those of the California Air Resources Board. The mention of commercial products, their source or their use in connection with material reported herein is not to be construed as either an actual or implied endorsement of such products.

Abstract

The principal objective of this research program was determination of the equilibrium distribution of pollutant materials between the gas and aerosol phases and of the subsequent relationships between the ambient aerosol and resultant visibility deterioration in the South Coast Air Basin of California. The Southern California Air Quality Study (SCAQS) data base was used extensively in addressing these two issues.

The question of whether equilibrium exists for ammonium nitrate between gas and aerosol phases in the atmosphere is important because in a polluted urban environment, the ammonium salts NH_4NO_3 and NH_4Cl account for 10–30% of the fine aerosol mass, and accurate prediction of the quantity of ammonium salts in the aerosol phase and their distribution with respect to particle size is essential to a full understanding of the source–receptor relations that govern the formation of the atmospheric aerosol.

By evaluating the time scales for equilibration of the vapor–phase species with a population of aerosol particles, we have found that ammonium salts in the gas and aerosol phases are not always in equilibrium, especially under less polluted and cooler conditions. Thus, both transport and thermodynamic properties of the aerosol population govern the distribution of ammonium salts.

To calculate the aerosol light scattering coefficient values via Mie theory aerosol size distribution data collected by the SCAQS air monitoring network have been combined with filter–based determinations of aerosol chemical composition.

It was found that the time series of the measured light scattering coefficient values could be reproduced well by the visibility model in those cases where redundant nephelometer measurements were available to assure that the measured light scattering coefficient values were not in doubt.

Acknowledgements

This report was submitted in fulfillment of ARB Contract A932-054, "Validity of Current Aerosol Models for Calculating Gas-Aerosol Equilibrium, Water Content, and Size Distributions and Relative Contribution of Various Source Types to Visibility," by the California Institute of Technology under the sponsorship of the California Air Resources Board. Work was completed as of April 13, 1992.

Contents

Abstract	iii
Table of Contents	v
List of Figures	vi
List of Tables	viii
1 The Distribution of Ammonium Salts among a Size and Composition Dispersed Aerosol	1
2 On the Interaction Between Equilibration Processes and Wet or Dry Deposition	17
3 Second-Generation Inorganic Aerosol Model	32
4 Analysis of Aerosol Ammonium Nitrate: Departures from Equilibrium during SCAQS	50
5 Visibility Modeling Using Continuous Aerosol Size Distribution Monitors	63
5.1 Introduction	63
5.2 Experimental Program	64
5.2.1 SCAQS Sampling	64
5.2.2 Aerosol Size Distributions	67
5.2.3 Aerosol Chemical Composition Measurements	67
5.2.4 Light Scattering Coefficient Data	71
5.2.5 Data Base Preparation	72
5.3 Correction of Aerosol Size Distribution Data Collected by the PMS Optical Particle Counter	74
5.4 Aerosol Volume Distributions	76
5.5 Creating a Combined Size Distribution for Use in Further Calculations	78
5.6 Internal Consistency of the Aerosol Chemistry Data Base	79
5.7 Estimation of the Aerosol Liquid Water Content	89
5.8 Estimation of Refractive Index	93
5.9 Calculation of the Extinction Coefficient	94
5.10 Visibility Model Results	96
5.11 Conclusions	103
References	110
Appendix A: Correction factors applied to the PMS OPC data	114

List of Figures

1	Southern California showing the locations of the aerosol size distribution monitoring network operated during SCAQS.	65
2	SCAQS sampler used for filter-based measurements of PM _{2.5} and PM ₁₀ aerosol mass concentrations and chemical composition.	69
3	Concurrent measurements of light scattering by particles made by different investigators during SCAQS. Dates are given as month, date (ie., 0619 is June 19, 1987).	73
4	An example of the raw size distribution data from the three size distribution monitors showing the extent of overlap between instruments.	77
5	An example of the final aerosol size distribution created for use in visibility modeling.	80
6	Anion and cation balance for PM _{2.5} at the Claremont site.	81
7	Anion and cation balance for PM ₁₀ at the Claremont site.	82
8	Anion and cation balance for PM _{2.5} at the Long Beach CC site.	83
9	Anion and cation balance for PM ₁₀ at the Long Beach CC site.	84
10	Anion and cation balance for PM _{2.5} at the Rubidoux site.	85
11	Anion and cation balance for PM ₁₀ at the Rubidoux site.	86
12	Anion and cation balance for the Central LA site during the fall.	87
13	Anion and cation balance for the Long Beach CC site during the fall.	88
14	Comparison of gravimetrically determined PM _{2.5} mass to the sum of the mass concentrations of identified chemical species.	90
15	Comparison of gravimetrically determined PM ₁₀ mass to the sum of the mass concentrations of identified chemical species.	91
16	Comparison of calculated light scattering by dry fine particles to nephelometer measurements of the particle light scattering coefficient (Case A).	98

17	Comparison of calculated light scattering by dry particles of 10 μm diameter and smaller to nephelometer measurements of the particle light scattering coefficient (Case B).	100
18	Comparison of calculated light scattering by particles to nephelometer measurements of the particle light scattering coefficient after having corrected the aerosol volume distributions to match the aerosol volume inferred from simultaneous filter samples (Case C).	101
19	Comparison of light scattering computed for a dry aerosol (Case C) to light scattering by a wetted aerosol (Case D).	104
20	Calculated values of the total light extinction coefficient for the Claremont site (Case C).	105
21	Calculated values of the total light extinction coefficient for the Long Beach CC site (Case C).	106
22	Calculated values of the total light extinction coefficient for the Rubidoux site (Case C).	107
23	Calculated values of the total light extinction coefficient for the Central LA and Long Beach CC sites in the fall (Case C).	108

List of Tables

1	Sites and Dates of SCAQS Intensive Field Experiments	66
2	Identification Numbers of Instruments used in the SCAQS Study Showing the Location of Particular Instruments during Different Seasons of the Year . . .	68
3	Dates and Times with Missing Data	75
4	Density and Refractive Index of Chemical Species	92
5	Methods Used to Calculate Alternative Refractive Index Values	95
6	Methods Used to Assign Size Distributions	97
7	Regression of Modeled Light Scattering Coefficient Values on Nephelometer Measurements of the Light Scattering Coefficient (all data)	102

THE DISTRIBUTION OF AMMONIUM SALTS AMONG A SIZE AND COMPOSITION DISPERSED AEROSOL

ANTHONY S. WEXLER

Department of Mechanical Engineering and Environmental Quality Laboratory, California Institute of
Technology, Pasadena, CA 91125, U.S.A.

and

JOHN H. SEINFELD

Department of Chemical Engineering, California Institute of Technology, Pasadena, CA 91125, U.S.A.

(First received 7 September 1989 and in final form 20 November 1989)

Abstract—The chemical and physical processes that govern the distribution of ammonium salt condensate over a size- and composition-dispersed aerosol particle population are considered. From an analysis of the concentration profiles of ammonia, nitric acid, and hydrochloric acid vapors surrounding an aerosol particle, the single particle fluxes of these species are derived. By evaluating the time scales for equilibration of the vapor-phase species with a population of aerosol particles, it is found that ammonium salts in the gas and aerosol phases are not always in equilibrium, especially under less polluted and cooler conditions. The principles that govern the distribution of ammonium salts on aerosol particles of different size and composition are identified, and it is found that thermodynamic equilibrium often does not uniquely determine the distribution of ammonium salt condensate. Thus it is concluded that both transport and thermodynamic properties of the aerosol population govern the distribution of ammonium salt condensate.

Key word index: Ammonium nitrate, ammonium chloride, atmospheric aerosol, thermodynamic equilibrium, aerosol size distribution, time constants.

INTRODUCTION

In a polluted urban environment, the ammonium salts NH_4NO_3 and NH_4Cl account for 10–30% of the fine aerosol mass, and the total inorganic salts account for 25–50% of the fine aerosol mass (Gray *et al.*, 1986; Heintzenberg, 1989). Stelson *et al.* (1979) postulate that these ammonium salts are in thermodynamic equilibrium with their vapor-phase components, NH_3 , HNO_3 and HCl . This equilibrium postulate is supported by ambient measurements (Hildemann *et al.*, 1984; Doyle *et al.*, 1979; Tanner, 1982; Grosjean, 1982), and the equilibrium constants for ammonium nitrate and ammonium chloride in the solid and aqueous phases have been calculated as a function of ambient temperature, relative humidity, and particle composition (Stelson *et al.*, 1979; Stelson and Seinfeld, 1982a; Pio and Harrison, 1987). A number of researchers (Russell *et al.*, 1983; Saxena *et al.*, 1983, 1986; Bassett and Seinfeld, 1983; Russell and Cass, 1986; Russell *et al.*, 1988) employ the equilibrium postulate to calculate the total mass of ammonium salt aerosol and others (Bassett and Seinfeld 1984; Pilinis *et al.*, 1987; Pilinis and Seinfeld, 1987, 1988) use an extension of this postulate to partition the condensed ammonium salts over a size- and composition-dispersed aerosol. Recently this postulate was questioned in an experimental investigation (Allen *et al.*, 1989).

Since accurate prediction of the quantity of ammonium salts in the aerosol phase and their distribution with respect to particle size is essential to a full understanding of the source-receptor relations that govern the formation of atmospheric aerosol, a study of the physical and chemical principles governing this partitioning is undertaken here. Atmospheric aerosol particles are considered to be composed of inorganic species in the solid and/or aqueous phases, perhaps coated by organic surface active agents. NH_3 , HNO_3 and HCl condense or evaporate from each particle depending on the relative concentrations of these species in the background gas and at the particle surface. The vapor-phase species are depleted from the gas phase in response to condensation on the aerosol particle, which results in a tendency for the particle population and the gas phase to equilibrate. Simultaneously, but at a slower rate, condensation and evaporation may occur such that individual aerosol particles tend to equilibrate with each other.

The analysis we are about to present is divided into three sections. To further our understanding of aerosol growth via condensation of ammonium salts, we first analyze the physical and chemical processes that govern transport of NH_3 and HX , the vapor-phase components of a general ammonium salt NH_4X , between the gas phase and a single aerosol particle. The processes that we consider are the reversible gas-

phase reaction $\text{NH}_4\text{X}(\text{g}) \rightleftharpoons \text{NH}_3(\text{g}) + \text{HX}(\text{g})$, the reversible particle surface accommodation reactions $\text{NH}_4\text{X}(\text{a}) \rightleftharpoons \text{NH}_3(\text{g}) + \text{HX}(\text{g})$ and $\text{NH}_4\text{X}(\text{a}) \rightleftharpoons \text{NH}_4\text{X}(\text{g})$, and diffusion of $\text{NH}_3(\text{g})$, $\text{HX}(\text{g})$ and $\text{NH}_4\text{X}(\text{g})$ between the background gas and the particle surface. By solving the differential equations that describe conservation of mass for the diffusing species, we obtain expressions for the net flux of NH_3 and HX to and from aerosol particles.

The equations describing the flux to a single particle enable us to answer a number of questions concerning populations of aerosol particles in the second section. We begin by identifying the characteristic times for a population of aerosol particles to equilibrate with the gas phase and, using these time scales, examine the atmospheric conditions under which the equilibrium assumption is valid. Next we identify the characteristics of aerosol particles that enable the equilibrium assumption to be used to partition ammonium salt condensate among the aerosol population. As a consequence, we also identify the characteristics of aerosol particles such that transport properties govern the distribution of ammonium salt condensate and equilibrium considerations play little or no role.

In the final section, we estimate the likely uncertainties in the relevant physical properties of aerosol particles and the resulting inherent uncertainty that we expect in the predicted size distribution of ammonium salts.

TRANSPORT OF $\text{NH}_3(\text{g})$, $\text{HNO}_3(\text{g})$ AND $\text{HCl}(\text{g})$ TO A SINGLE PARTICLE

Let us consider the equations governing mass transport of NH_3 and HX , the vapor-phase components of a general ammonium salt NH_4X , between gas and aerosol phases. The physical and chemical processes that we consider are (1) molecular diffusion of the gas-phase species $\text{NH}_3(\text{g})$, $\text{HX}(\text{g})$ and $\text{NH}_4\text{X}(\text{g})$, (2) the reversible gas-phase reaction $\text{NH}_3(\text{g}) + \text{HX}(\text{g}) \rightleftharpoons \text{NH}_4\text{X}(\text{g})$, and (3) the surface reactions $\text{NH}_3(\text{g}) + \text{HX}(\text{g}) \rightleftharpoons \text{NH}_4\text{X}(\text{a})$ and $\text{NH}_4\text{X}(\text{g}) \rightleftharpoons \text{NH}_4\text{X}(\text{a})$, where $\text{NH}_4\text{X}(\text{a})$ is an ammonium salt in the aqueous or solid aerosol phase.

The transport of $\text{NH}_3(\text{g})$, $\text{HX}(\text{g})$, and $\text{NH}_4\text{X}(\text{g})$ between the gas and an aerosol particle is governed by the differential equations for mass conservation in the gas phase

$$\begin{aligned} \frac{\partial C_{\text{NH}_4\text{X}}}{\partial t} - \frac{D_{\text{NH}_4\text{X}}}{r^2} \frac{\partial}{\partial r} \left(r^2 \frac{\partial C_{\text{NH}_4\text{X}}}{\partial r} \right) \\ = - \frac{\partial C_{\text{NH}_3}}{\partial t} + \frac{D_{\text{NH}_3}}{r^2} \frac{\partial}{\partial r} \left(r^2 \frac{\partial C_{\text{NH}_3}}{\partial r} \right) \\ = - \frac{\partial C_{\text{HX}}}{\partial t} + \frac{D_{\text{HX}}}{r^2} \frac{\partial}{\partial r} \left(r^2 \frac{\partial C_{\text{HX}}}{\partial r} \right) \\ = k_+ C_{\text{NH}_3} C_{\text{HX}} - k_- C_{\text{NH}_4\text{X}} \end{aligned}$$

where C_i are the gas-phase concentrations, D_i are the molecular diffusivities, t is time, r is the radial distance from the center of the aerosol particle with radius R_p , and k_+ and k_- are the forward and reverse rate constants for the reversible gas-phase reaction. We proceed in steps to consider the magnitude of each of the terms in this equation and then to solve it. The first step is to consider the time derivative terms.

Gas-phase diffusion and reaction time scales

Let us consider a solid- or aqueous-phase particle of NH_4X in chemical equilibrium with the surrounding gas-phase. Suppose the concentrations of either or both of the gas-phase species, $\text{NH}_3(\text{g})$ and $\text{HX}(\text{g})$, far from the particle are instantaneously increased, resulting in condensation on the particle as new equilibrium conditions are approached. The initial changes in the gas-phase concentrations far from the particle are propagated toward the particle until a steady state concentration profile is established. There are two time scales associated with this relaxation to a steady state profile: one associated with the time, τ_D , required for the gas-phase concentration profile to reach a steady state by molecular diffusion, and the other associated with the time, τ_K , required for the concentration profile to reach a steady state with respect to the reversible gas-phase chemical reaction.

We assume that far from the particle the gas-phase concentrations of NH_3 and HX are known and that at the particle surface there is condensation of these species. For species that do not undergo a significant gas-phase reaction, the characteristic time for establishment of the steady state profile due to molecular diffusion is $\tau_D \sim R_p^2/D_i$ (Seinfeld, 1986), which under typical atmospheric conditions and particle size is less than 10^{-6} s.

The characteristic time for equilibration of the gas-phase reaction $\text{NH}_3(\text{g}) + \text{HX}(\text{g}) \rightleftharpoons \text{NH}_4\text{X}(\text{g})$ is $\tau_K = [k_+(C_{\text{NH}_3,e} + C_{\text{HX},e}) + k_-]^{-1}$, where $C_{\text{NH}_3,e}$ and $C_{\text{HX},e}$ are the equilibrium concentrations of the gas-phase species (Hill, 1977). Since the equilibrium constant is given by $K_{\text{NH}_4\text{X}(\text{g})} = k_-/k_+$, we can express this time scale as

$$\tau_K = \frac{1/k_+}{C_{\text{NH}_3,e} + C_{\text{HX},e} + K_{\text{NH}_4\text{X}(\text{g})}}$$

Determination of the equilibrium constant, $K_{\text{NH}_4\text{Cl}(\text{g})}$, for the reaction $\text{NH}_3(\text{g}) + \text{HCl}(\text{g}) \rightleftharpoons \text{NH}_4\text{Cl}(\text{g})$ was an active area of research around the turn of the century. Most of the investigations were carried out at temperatures much higher than atmospheric (see Table 1). The data concerning the dissociation of NH_4Cl are usually expressed in terms of the dissociation constant, $b_{\text{NH}_4\text{Cl}}$, for the reaction

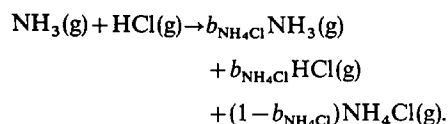


Table 1. Dissociation constant and equilibrium constant of $\text{NH}_4\text{Cl}(\text{g})$

Investigator	Temperature (K)	$b_{\text{NH}_4\text{Cl}(\text{g})}$ (%)	K_p (atm)
Ramsay and Young (1886)	553	70–80	—
Smith and Lombard (1915)	> 553	60–70	3×10^{-7} at 300 K*
Rodebush and Michalek (1929)	562	100	—
Stephenson (1944)	—	100	—
Clementi and Gayles (1967)	< 2000	100	1.3×10^{-4} at 300 K*
Shibata (1970)	523	~ 60	—
de Kruif (1982)	352	85	1×10^{-5}

* Inferred from data available in these papers.

The equilibrium constant can be expressed in terms of the dissociation constant as

$$K_{\text{NH}_4\text{Cl}(\text{g})} \equiv \frac{p_{\text{NH}_3} p_{\text{HCl}}}{p_{\text{NH}_4\text{Cl}}} = \frac{b_{\text{NH}_4\text{Cl}}^2}{1 - b_{\text{NH}_4\text{Cl}}^2} p_t$$

where p_t is the total pressure of $\text{NH}_3(\text{g})$, $\text{HCl}(\text{g})$ and $\text{NH}_4\text{Cl}(\text{g})$ (de Kruif, 1982).

There are no reported measurements of the dissociation constant of $\text{NH}_4\text{Cl}(\text{g})$ at typical atmospheric temperatures and pressures. At elevated temperatures and somewhat lower pressures numerous measurements and calculations have been performed and are in substantial disagreement. Since the data of de Kruif (1982) are by far the closest to atmospheric temperature of any of the measurements or computations in the literature and since he finds that the dissociation constant is relatively insensitive to temperature, we use 85% as the dissociation constant of NH_4Cl at 352 K along with the total pressure of 0.4 Pa to obtain

$$K_{\text{NH}_4\text{Cl}(\text{g})} = 1 \times 10^{-5} \text{ atm}$$

under atmospheric conditions.

In the same set of experiments, de Kruif (1982) finds the dissociation constant for $\text{NH}_4\text{NO}_3(\text{g})$ at 352 K to be 66%. Again assuming that the dissociation constant is a weak function of temperature along with the measured total pressure of 0.40 Pa, we find

$$K_{\text{NH}_4\text{NO}_3(\text{g})} \equiv \frac{p_{\text{NH}_3} p_{\text{HNO}_3}}{p_{\text{NH}_4\text{NO}_3}} = 3 \times 10^{-6} \text{ atm.}$$

We can estimate the maximum likely concentration of $\text{NH}_4\text{Cl}(\text{g})$ and $\text{NH}_4\text{NO}_3(\text{g})$ by assuming that the maximum concentration of the dissociated species are each 100 ppb. Using these concentrations with the equilibrium constants $K_{\text{NH}_4\text{Cl}(\text{g})}$ and $K_{\text{NH}_4\text{NO}_3(\text{g})}$ results in $p_{\text{NH}_4\text{Cl}} = 1$ ppb and $p_{\text{NH}_4\text{NO}_3} = 3$ ppb. A more typical concentration for the dissociated species is 10 ppb, which results in $p_{\text{NH}_4\text{Cl}} = 0.01$ ppb and $p_{\text{NH}_4\text{NO}_3} = 0.03$ ppb. Thus we find that under atmospheric conditions the concentration of the associated species is considerably less than the concentrations of the dissociated species. This is used in a later section when the boundary conditions are developed.

Returning to evaluation of τ_K , under typical atmospheric conditions the concentrations of $\text{NH}_3(\text{g})$, $\text{HCl}(\text{g})$ and $\text{HNO}_3(\text{g})$ are considerably less than the values of $K_{\text{NH}_4\text{Cl}(\text{g})}$ and $K_{\text{NH}_4\text{NO}_3(\text{g})}$, so the time constant for the concentration profiles to reach steady state due to the reaction $\text{NH}_3(\text{g}) \pm \text{HX}(\text{g}) \rightleftharpoons \text{NH}_4\text{X}(\text{g})$ can be simplified to

$$\tau_K \sim \frac{1}{k_+ K_{\text{NH}_4\text{X}(\text{g})}}$$

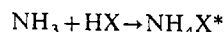
To evaluate the time constant, τ_K , for the reaction to reach steady state, the values of the forward or reverse rate constants for these reactions are needed. Countess and Hecklen (1973) measured the number concentration of $\text{NH}_4\text{Cl}(\text{s})$ particles formed in a nucleation experiment. From the initial rate of particle formation, they infer the forward rate constant to be $k_+ = 467 \text{ atm}^{-1} \text{ s}^{-1}$. In a check of this rate constant, they measured the rate of disappearance of $\text{NH}_3(\text{g})$ from a batch reactor containing $\text{NH}_3(\text{g})$, $\text{HCl}(\text{g})$ and $\text{N}_2(\text{g})$. Also in a nucleation experiment, Henry *et al.* (1983) find double the value of this rate constant fit their data better.

An upper limit for k_+ for NH_4X is given by the collision rate:

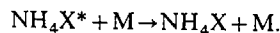
$$k_+ \leq \sqrt{\frac{8kT}{\pi\mu}} \frac{\pi\sigma^2}{kT}$$

where k is the Boltzmann constant, T is the temperature, $\mu = 1.93 \times 10^{-26} \text{ kg molecule}^{-1}$ and $\pi\sigma^2 = 1.5 \times 10^{-19} \text{ m}^2$ are the reduced mass and cross-section for NH_3 and HCl collisions, while $\mu = 2.23 \times 10^{-26} \text{ kg molecule}^{-1}$ and $\pi\sigma^2 = 1.8 \times 10^{-19} \text{ m}^2$ are the same quantities for NH_3 and HNO_3 collisions. Evaluating this expression at 298 K gives $k_+ \leq 2.7 \times 10^9 \text{ atm}^{-1} \text{ s}^{-1}$ for NH_4Cl and $k_+ \leq 3.0 \times 10^9 \text{ atm}^{-1} \text{ s}^{-1}$ for NH_4NO_3 . Clementi and Gayles (1967) predict that the energy barrier for the reaction forming $\text{NH}_4\text{Cl}(\text{g})$ is small, which suggests that the collision theory estimate may not be too many orders of magnitude from the actual value. There are a number of possible explanations for the large discrepancy between the three measured values and the maximum value calculated from collision theory.

The rate constant based on collision theory is high because the actual reaction probably requires a third molecule, M, to stabilize the $\text{NH}_4\text{X}(\text{g})$ molecule:



followed by



In both experiments the total pressures are nearly atmospheric, so concentrations of M are representative of atmospheric values. The experimental data may be low simply due to limitations in the rate of mixing of the two gas streams, as in both experiments the flow was laminar; thus the measured reaction rate may not be limited by the chemical kinetics but rather by the rate of diffusion.

Using the equilibrium and rate constants, we can evaluate the time constant for the gas-phase concentration profiles to reach steady state due to the gas-phase chemical reaction. For the forward rate constant based on collision theory, we obtain $\tau_k > 10^{-5}$ s, and for the forward rate constant based on the experimental data of Countess and Hecklen (1973) and Henry *et al.* (1983), we obtain $\tau_k \sim 3.5$ min.

Either characteristic time is probably short compared to those of the other processes affecting the ambient concentrations of $\text{NH}_3(\text{g})$, $\text{HX}(\text{g})$ and $\text{NH}_4\text{X}(\text{g})$. We assume this is the case and thus that transport of $\text{NH}_3(\text{g})$ and $\text{HX}(\text{g})$ to and from an aerosol particle in response to changes in background gas-phase concentrations occurs with the gas-phase concentration profiles in steady state. This assumption is supported by other findings in a later section.

For aqueous-phase particles there are additional time scales related to (1) attaining interfacial equilibrium and (2) diffusion in the liquid phase. For the species being considered here, both of these time scales are less than 1 s (Seinfeld, 1986).

Thus the gas-phase concentration profiles of $\text{NH}_3(\text{g})$, $\text{HX}(\text{g})$ and $\text{NH}_4\text{X}(\text{g})$ are governed by the steady state form of the continuity equation

$$\begin{aligned} \frac{D_{\text{NH}_4\text{X}}}{r^2} \frac{d}{dr} \left(r^2 \frac{dC_{\text{NH}_4\text{X}}}{dr} \right) &= - \frac{D_{\text{NH}_3}}{r^2} \frac{d}{dr} \left(r^2 \frac{dC_{\text{NH}_3}}{dr} \right) \\ &= - \frac{D_{\text{HX}}}{r^2} \frac{d}{dr} \left(r^2 \frac{dC_{\text{HX}}}{dr} \right) \\ &= k_- C_{\text{NH}_4\text{X}} - k_+ C_{\text{NH}_3} C_{\text{HX}}. \end{aligned}$$

It is worth emphasizing here that although the gas-phase concentrations are in steady-state they are not necessarily in chemical equilibrium. In the vicinity of the particle, molecular diffusion to and from the particle perturbs the gas-phase concentrations, driving the species out of equilibrium, while the reversible chemical reaction $\text{NH}_4\text{X}(\text{g}) \rightleftharpoons \text{NH}_3(\text{g}) + \text{HX}(\text{g})$ drives these concentrations toward equilibrium. Steady-state is reached when molecular diffusion and chemical reaction balance.

The diffusion-reaction length scale

If we non-dimensionalize the above differential equation, we find that the characteristic thickness of the diffusion-reaction boundary layer surrounding the particle is

$$\lambda = \sqrt{D_{\text{NH}_4\text{X}}/k_-} \equiv \sqrt{D_{\text{NH}_4\text{X}}/K_{\text{NH}_4\text{X}(\text{g})}k_+}.$$

The square of the ratio of the particle radius over the diffusion-reaction boundary layer thickness is the so called Damköhler number, $\gamma = R_p^2/\lambda^2$ (Schultz *et al.*, 1974). When there are no gas-phase reactions, $\text{NH}_3(\text{g}) + \text{HX}(\text{g}) \rightleftharpoons \text{NH}_4\text{X}(\text{g})$, the concentration profile is governed exclusively by molecular diffusion, λ is infinite, and γ is zero. When k_- and k_+ are small but non-zero, λ is large, γ is small, and the gas-phase reaction slightly perturbs the concentration profile due to molecular diffusion alone. When k_- and k_+ are large, λ is small, γ is large, and the gas-phase reactions have a significant effect upon the concentration profiles. These three cases are illustrated qualitatively in Fig. 1.

Before we proceed, let us try to obtain a greater physical understanding of the diffusion-reaction boundary layer thickness, λ . Imagine a control volume surrounding the particle and encompassing this boundary layer. There are two competing processes that are at balance within the control volume: the gas-phase chemical reaction, which drives the local concentrations toward equilibrium, and molecular diffusion of the gas-phase species through the surface of the control volume, which drives the concentrations out of chemical equilibrium. The thickness of the diffusion-reaction boundary layer defines a spherical shell surrounding the particle where in a qualitative sense the molecular diffusion through the surface of the shell balances the gas-phase chemical reactions occurring within the volume of the shell.

To illustrate the effect of the gas-phase reaction, let us consider condensation of $\text{NH}_3(\text{g})$, $\text{HX}(\text{g})$ and $\text{NH}_4\text{X}(\text{g})$ on a solid NH_4X particle. If, for example,

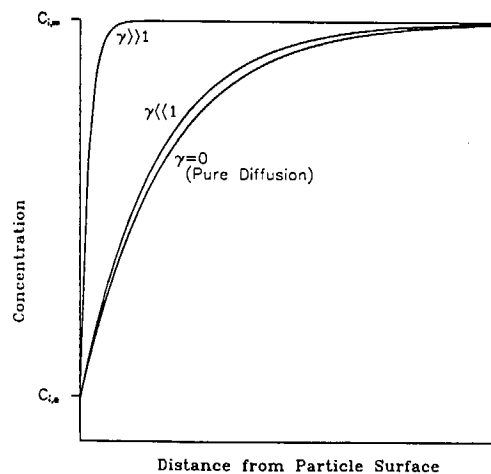


Fig. 1. Typical concentration profile as a function of Damköhler number, γ .

surface accommodation is via NH_4X only, and if the Damköhler number is large, $\text{NH}_3(\text{g})$ and $\text{HX}(\text{g})$ will diffuse toward the particle along with $\text{NH}_4\text{X}(\text{g})$. In the thin boundary layer near the particle surface, the reaction $\text{NH}_3(\text{g}) + \text{HX}(\text{g}) \rightarrow \text{NH}_4\text{X}(\text{g})$ takes place, and the $\text{NH}_4\text{X}(\text{g})$ is accommodated. Without the chemical reaction, only diffusion of $\text{NH}_4\text{X}(\text{g})$ may contribute to overall transport to the particle, since there is no gas-phase mechanism for forming NH_4X and only NH_4X can be accommodated, but with the chemical reaction, the overall transport is augmented by diffusion of $\text{NH}_3(\text{g})$ and $\text{HX}(\text{g})$ toward the particle in addition to the diffusion of $\text{NH}_4\text{X}(\text{g})$.

If the Damköhler number is small, an insufficient amount of $\text{NH}_3(\text{g})$ and $\text{HX}(\text{g})$ are converted to $\text{NH}_4\text{X}(\text{g})$ in the vicinity of the particle to affect the gas-phase concentration profiles or the overall transport. Furthermore, if accommodation is via $\text{NH}_3(\text{g})$ and $\text{HX}(\text{g})$ instead of $\text{NH}_4\text{X}(\text{g})$, even a large Damköhler number does not have a significant effect on the concentration profiles or the transport because under typical atmospheric conditions the concentrations of $\text{NH}_3(\text{g})$ and $\text{HX}(\text{g})$ are considerably greater than the concentration of $\text{NH}_4\text{X}(\text{g})$. We will now estimate the magnitude of the Damköhler number and, in the following section, the mode of accommodation onto solid and aqueous-phase particles.

The length of the diffusion-reaction boundary layer can be expressed in terms of the characteristic time for the gas-phase reaction as $\lambda = \sqrt{D_{\text{NH}_4\text{X}} \tau_K}$. Assuming that $D_{\text{NH}_4\text{X}} \sim 10^{-5} \text{ m}^2 \text{ s}^{-1}$, this expression can be evaluated at the τ_K value obtained from the experimentally determined kinetics of Countess and Heicklen (1973) and Henry *et al.* (1983) to obtain $\lambda \sim 5 \text{ cm}$, or at the collision theory value of τ_K to obtain $\lambda > 10 \text{ } \mu\text{m}$. Thus, for both of these time constant values we find that the Damköhler number, γ , is probably much less than unity, and we are led to the conclusion that, at the size of typical atmospheric aerosol particles, diffusion governs the concentration profiles surrounding the particle.

We have now determined that the concentration profile surrounding the particle is in steady state and that the gas-phase reaction $\text{NH}_3(\text{g}) + \text{HX}(\text{g}) \rightleftharpoons \text{NH}_4\text{X}(\text{g})$ does not significantly affect these concentration profiles. The resulting continuity equations governing the concentrations are

$$\begin{aligned} \frac{D_{\text{NH}_4\text{X}}}{r^2} \frac{d}{dr} \left(r^2 \frac{dC_{\text{NH}_4\text{X}}}{dr} \right) &= - \frac{D_{\text{NH}_3}}{r^2} \frac{d}{dr} \left(r^2 \frac{dC_{\text{NH}_3}}{dr} \right) \\ &= - \frac{D_{\text{HX}}}{r^2} \frac{d}{dr} \left(r^2 \frac{dC_{\text{HX}}}{dr} \right) = 0. \end{aligned}$$

To solve the equations, we now develop the boundary conditions.

Accommodation of NH_3 , HX and NH_4X on the particle surface

$\text{NH}_3(\text{g})$, $\text{HX}(\text{g})$ and $\text{NH}_4\text{X}(\text{g})$ can sublime or condense on the particle surface according to the reac-

tions $\text{NH}_3(\text{g}) + \text{HX}(\text{g}) \rightleftharpoons \text{NH}_4\text{X}(\text{s})$, $\text{NH}_3(\text{g}) \rightleftharpoons \text{NH}_3(\text{aq})$, $\text{HX}(\text{g}) \rightleftharpoons \text{HX}(\text{aq})$, or $\text{NH}_4\text{X}(\text{g}) \rightleftharpoons \text{NH}_4\text{X}(\text{a})$. Since the concentration of $\text{NH}_4\text{X}(\text{g})$ is considerably less than the concentrations of $\text{NH}_3(\text{g})$ and $\text{HX}(\text{g})$, the predicted rate of mass transport to and from the particle may differ by an order of magnitude or more, depending on whether sublimation and condensation is via the associated or dissociated species. Also, the rate of this accommodation reaction governs whether the accommodation rate or gas-phase diffusion dominates transport to and from the particle. We will now address these questions.

Chaiken *et al.* (1962) measure the sublimation rate of $\text{NH}_4\text{Cl}(\text{s})$ tablets and strands and find results in agreement with those of Schultz and Dekker (1956) in the temperature range 420–1000 K, giving an Arrhenius form of the sublimation rate, B , in terms of the rate of change of the particle radius:

$$B = 0.6 \exp \left(\frac{-13,200 \text{ cal mol}^{-1}}{RT} \right) [\text{m s}^{-1}].$$

Sturges and Harrison (1988) measure the evaporation rate of solid NH_4Cl particles and find $B = 1.3 \times 10^{-10} \text{ m s}^{-1}$. Unfortunately, they do not state the temperature at which the experiment was performed, but imply 293 K. Evaluating Chaiken's expression at 293 K gives $B = 0.85 \times 10^{-10} \text{ m s}^{-1}$ and at 298 K gives $B = 1.25 \times 10^{-10} \text{ m s}^{-1}$, which are both in excellent agreement with the Sturges and Harrison value.

Schultz and Dekker (1956) propose that the dissociation $\text{NH}_4\text{Cl} \rightarrow \text{NH}_3 + \text{HCl}$ occurs on the surface of $\text{NH}_4\text{Cl}(\text{s})$ so that dissociated vapor leaves the solid during sublimation. This proposal is confirmed by Tang and Fenn (1973) at 358 K. Countess and Heicklen (1973) and Dahlin *et al.* (1981) infer that nucleation and condensation occur via the associated species so that the surface reaction is $\text{NH}_4\text{Cl}(\text{g}) \rightarrow \text{NH}_4\text{Cl}(\text{s})$. Since the sublimation experiments were carried out at elevated temperatures and the nucleation experiments at elevated concentrations compared to typical atmospheric conditions, we are left with an indefinite conclusion regarding the appropriate mode for the surface reaction.

If we assume that the accommodation reaction occurs via the dissociated species, we can estimate the maximum sublimation rate from kinetic theory. The maximum condensation rate occurs when every NH_3 and HCl molecule that strikes the particle surface is accommodated. Then the maximum rate of condensation, R_{max} , is governed by the species with the lower rate of collision with the particle:

$$R_{\text{max}} = \sqrt{\frac{8kT}{\pi m_{\text{NH}_3}}} \min \left(\frac{p_{\text{NH}_3}}{RT}, \sqrt{\frac{m_{\text{NH}_3}}{m_{\text{HCl}}}} \frac{p_{\text{HCl}}}{RT} \right),$$

where m_{NH_3} and m_{HCl} are the masses of the corresponding molecules. For $p_{\text{NH}_3} = p_{\text{HCl}}$, which corresponds to most of the experimental data,

$$R_{\text{max}} = \sqrt{\frac{8kT}{\pi m_{\text{HCl}}}} \frac{p_{\text{HCl}}}{RT}.$$

If the gas phase is not far from equilibrium with the aerosol phase, the partial pressure of $\text{HCl}(\text{g})$ is approximately the equilibrium partial pressure, $p_{\text{HCl}} \sim \sqrt{K_{\text{NH}_4\text{Cl}(\text{s})}}$. Pio and Harrison (1987) calculate the equilibrium constant, $K_{\text{NH}_4\text{Cl}(\text{s})} \equiv p_{\text{NH}_3} p_{\text{HCl}}$, for this reaction from accepted thermodynamic data and find

$$\begin{aligned} \ln K_{\text{NH}_4\text{Cl}(\text{s})} = & 2.2358 \ln\left(\frac{T}{298}\right) - \frac{21,320}{T} + 36.729 \\ & - 8.167 \times 10^{-3} T + 4.644 \times 10^{-7} T^2 \\ & - 1.105 \times 10^{-10} T^3 \end{aligned}$$

where $K_{\text{NH}_4\text{Cl}(\text{s})}$ is in atm^2 .

Near equilibrium the condensation rate is approximately the same as the sublimation rate, $R_{\text{max}} \sim B_{\text{max}}$, and we find

$$B_{\text{max}} \sim \sqrt{\frac{8kT}{\pi m_{\text{HCl}}}} \sqrt{\frac{K_{\text{NH}_4\text{Cl}(\text{s})}}{RT}}$$

Evaluating this expression at 298 K gives $B_{\text{max}} = 59 \times 10^{-10} \text{ m s}^{-1}$, a factor of 45 higher than the observed rate.

If we now assume that the accommodation occurs via $\text{NH}_4\text{Cl}(\text{g})$, we can use the assumption that the gas phase is not far from equilibrium with the aerosol phase in order to estimate the maximum sublimation rate:

$$R_{\text{max}} = \sqrt{\frac{8kT}{\pi m_{\text{NH}_4\text{Cl}}}} \frac{p_{\text{NH}_4\text{Cl}}}{RT}$$

Near equilibrium, we have $p_{\text{NH}_4\text{Cl}} = K_{\text{NH}_4\text{Cl}(\text{s})}/K_{\text{NH}_4\text{Cl}(\text{g})} = 6.9 \times 10^{-12} \text{ atm}$ at 298 K. Evaluating R_{max} at 298 K gives $B_{\text{max}} = 0.035 \times 10^{-10} \text{ m s}^{-1}$, a factor of 30 lower than the observed rate. Thus we are able to eliminate $\text{NH}_4\text{Cl}(\text{g}) \rightleftharpoons \text{NH}_4\text{Cl}(\text{s})$ as the gas-solid aerosol accommodation mechanism under atmospheric temperature and pressure.

There are far less data available for sublimation of $\text{NH}_4\text{NO}_3(\text{s})$ than are available for $\text{NH}_4\text{Cl}(\text{s})$. Andersen *et al.* (1958) measure the evaporation rate of $\text{NH}_4\text{NO}_3(\text{s})$ strands at surface temperatures above the melting point, 443 K, using the same procedures employed by Chaiken *et al.* (1962) for NH_4Cl . The data fit the Arrhenius form, but a sharp change in the kinetics occurs in the neighbourhood of the melting point—a not unexpected finding—and insufficient data were obtained below the melting point to arrive at a sublimation rate. It is clear from their data that the sublimation rate expressed in terms of the rate of change of particle radius is many orders of magnitude lower than 10^{-6} m s^{-1} at atmospheric temperatures.

Richardson and Hightower (1987) measure the sublimation rate of solid ammonium nitrate particles and find the rate to be initially $0.23 \times 10^{-10} \text{ m s}^{-1}$, but after 4 h it is only $0.06 \times 10^{-10} \text{ m s}^{-1}$. Later these same investigators (Hightower and Richardson, 1988) obtain a rate of about $0.4 \times 10^{-10} \text{ m s}^{-1}$ with mixed ammonium nitrate-ammonium sulfate salts and a value of $22 \times 10^{-10} \text{ m s}^{-1}$ when extrapolated to pure

NH_4NO_3 . When these particles were exposed to relative humidities of 20–60%, the rate for mixed salts was about $4 \times 10^{-10} \text{ m s}^{-1}$.

Let us assume that dissociation into NH_3 and HNO_3 occurs at the particle surface and that the equilibrium constant is not changed substantially by the NH_4NO_3 being in the same crystal lattice or solid solution with $(\text{NH}_4)_2\text{SO}_4$. We can then evaluate the expression for the maximum sublimation rate using the equilibrium constant (Stelson *et al.*, 1979)

$$\ln K_{\text{NH}_4\text{NO}_3(\text{s})} = 43.054 - \frac{24,110}{T} - 5.93 \ln\left(\frac{T}{298.15}\right),$$

where $K_{\text{NH}_4\text{NO}_3(\text{s})} \equiv p_{\text{NH}_3} p_{\text{HNO}_3}$ is in atm^2 , to obtain $B_{\text{max}} = 36 \times 10^{-10} \text{ m s}^{-1}$, 1.5–600 times higher than the observed rates.

If we assume the accommodation occurs via $\text{NH}_4\text{NO}_3(\text{g})$ and the gas and solid phases are not far from equilibrium, the maximum sublimation rate is $B_{\text{max}} = 0.065 \times 10^{-10} \text{ m s}^{-1}$ at 298 K, which corresponds to the lowest reported experimental value. Although the case is not as conclusive here as for ammonium chloride, we conclude that the mechanism for accommodation is most likely $\text{NH}_3(\text{g}) + \text{HNO}_3(\text{g}) \rightleftharpoons \text{NH}_4\text{NO}_3(\text{s})$.

The laboratory data of Hightower and Richardson (1988) suggest a unity accommodation coefficient for $\text{NH}_3(\text{g})$ and $\text{HNO}_3(\text{g})$ on aqueous-phase particles. Under atmospheric conditions, Gill *et al.* (1983) suggest that aerosol particles are likely to be completely coated by organic surface active agents that reduce the sticking coefficient of water molecules on water to 1/300 or less. In a subsequent work (Graedel *et al.*, 1983), a sticking coefficient of 1/500 for other atmospheric constituents is assumed. If we assume that the sticking coefficient is relatively independent of which species is being accommodated, transport to and from the aqueous phase is dominated by $\text{NH}_3(\text{g})$ and $\text{HX}(\text{g})$, since their gas-phase concentrations are much higher than those of $\text{NH}_4\text{X}(\text{g})$. Thus we can conclude that sublimation and condensation occur primarily via the dissociated species for both solid- and aqueous-phase aerosol particles.

For solid particles, the experimentally determined surface rate constants are 10–50 times smaller than the value based on collision theory, and thus we assume that the accommodation coefficient is in the range of 1/10–1/50 for solid particles. For aqueous-phase particles, we will explore the effect of the accommodation coefficient on transport, considering values between 1 and 1/500. Since (1) accommodation is via the dissociated species and (2) the gas-phase reactions do not significantly affect the concentration profiles, the concentration profile of $\text{NH}_4\text{X}(\text{g})$ does not affect the transport process. These conclusions also support the steady state assumption made earlier. The continuity equations can be further simplified to

$$\frac{D_{\text{NH}_3}}{r^2} \frac{d}{dr} \left(r^2 \frac{dC_{\text{NH}_3}}{dr} \right) = \frac{D_{\text{HX}}}{r^2} \frac{d}{dr} \left(r^2 \frac{dC_{\text{HX}}}{dr} \right) = 0.$$

The boundary conditions for this differential equation state that (1) far from the particle the concentrations of $\text{NH}_3(\text{g})$ and $\text{HX}(\text{g})$ are known

$$C_{\text{NH}_3}(r \rightarrow \infty) = C_{\text{NH}_3, \infty}$$

$$C_{\text{HX}}(r \rightarrow \infty) = C_{\text{HX}, \infty}$$

and (2) at the particle surface, surface reactions govern the accommodation of only the dissociated species, $\text{NH}_3(\text{g})$ and $\text{HX}(\text{g})$, into the aerosol phase. For solid-phase particles, the flux of NH_3 must balance the flux of HX so the boundary conditions are

$$D_{\text{NH}_3} \frac{dC_{\text{NH}_3}}{dr} \Big|_{r=R_p} = D_{\text{HX}} \frac{dC_{\text{HX}}}{dr} \Big|_{r=R_p}$$

$$= \alpha k_{\text{coll}, \text{NH}_4\text{X}(\text{s})} (C_{\text{NH}_3}(R_p) C_{\text{HX}}(R_p) - K_{\text{NH}_4\text{X}(\text{s})}),$$

where $k_{\text{coll}, \text{NH}_4\text{X}(\text{s})}$ is the collision-limited surface reaction rate constant and α is the sticking coefficient. For aqueous-phase particles, the boundary conditions are

$$D_{\text{NH}_3} \frac{dC_{\text{NH}_3}}{dr} \Big|_{r=R_p} = \alpha k_{\text{coll}, \text{NH}_3} (C_{\text{NH}_3}(R_p) - C_{e, \text{NH}_3})$$

$$D_{\text{HX}} \frac{dC_{\text{HX}}}{dr} \Big|_{r=R_p} = \alpha k_{\text{coll}, \text{HX}} (C_{\text{HX}}(R_p) - C_{e, \text{HX}})$$

and $k_{\text{coll}, i}$ is the mean speed of molecules of the condensing vapor-phase species, NH_3 and HX .

The appropriate non-dimensionalization of these boundary conditions yields for solid particles

$$\sqrt{\frac{D_{\text{NH}_3} \beta_{\text{NH}_4\text{X}(\text{s})}}{D_{\text{HX}} \bar{C}}} \frac{dC_{\text{NH}_3}}{d\rho} \Big|_{\rho=1} = \sqrt{\frac{D_{\text{HX}} \beta_{\text{NH}_4\text{X}(\text{s})}}{D_{\text{NH}_3} \bar{C}}} \frac{dC_{\text{HX}}}{d\rho} \Big|_{\rho=1}$$

$$= \frac{C_{\text{NH}_3}(\rho=1) C_{\text{HX}}(\rho=1) - K_{\text{NH}_4\text{X}(\text{s})}}{\bar{C}^2},$$

where $\beta_{\text{NH}_4\text{X}(\text{s})} = \sqrt{D_{\text{NH}_3} D_{\text{HX}} / \alpha k_{\text{coll}, \text{NH}_4\text{X}(\text{s})} R_p \bar{C}}$ is the dimensionless surface accommodation factor which indicates whether gas-phase diffusion or surface accommodation limit transport to and from a solid particle, $\rho = r/R_p$ is the dimensionless radial coordinate, and $\bar{C} = (D_{\text{NH}_3} C_{\text{NH}_3, \infty} + D_{\text{HX}} C_{\text{HX}, \infty}) / \sqrt{D_{\text{NH}_3} D_{\text{HX}}}$ is a diffusion weighted average of the concentrations far from the particle. For aqueous-phase particles, non-dimensionalizing yields

$$\beta_{\text{NH}_3} \frac{dC_{\text{NH}_3}}{d\rho} \Big|_{\rho=1} = C_{\text{NH}_3}(\rho=1) - C_{e, \text{NH}_3}$$

$$\beta_{\text{HX}} \frac{dC_{\text{HX}}}{d\rho} \Big|_{\rho=1} = C_{\text{HX}}(\rho=1) - C_{e, \text{HX}}$$

where $\beta_i = D_i / \alpha k_{\text{coll}, i} R_p$ is the surface accommodation factor for aqueous-phase particles. If α is unity, every molecule that strikes the particle surface is accommodated, and β_i is at its minimum for a given species. Transport to the particle must be limited by diffusion, since surface accommodation is ideal. As α decreases, β_i increases, and the transport of species to the particle

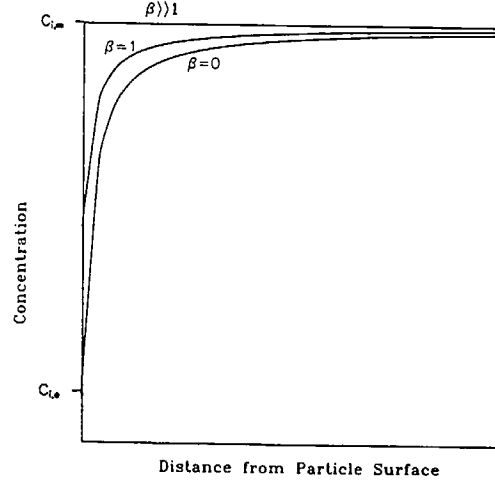


Fig. 2. Typical concentration profile as a function of surface accommodation factor, β .

becomes more limited by the surface accommodation. Eventually, α is so small that diffusion no longer limits transport and the vapor concentration profiles surrounding the particle are flat (see Fig. 2). As will be seen in subsequent derivations, when $\beta_i \sim 1$, both diffusion and surface accommodation affect transport to the particle.

Evaluating $\bar{D} / \alpha k_{\text{coll}, \text{NH}_4\text{X}(\text{s})} \sqrt{K_{\text{NH}_4\text{X}(\text{s})}}$ for $\text{NH}_4\text{Cl}(\text{s})$ gives $\sim 0.5 \mu\text{m}$, whereas evaluating it for $\text{NH}_4\text{NO}_3(\text{s})$ gives $0.01\text{--}10 \mu\text{m}$. For aqueous-phase particles with surface accommodation coefficient, α , in the range $0.1\text{--}0.01$, we find $D_i / \alpha k_{\text{coll}, i}$ in the range of $0.3\text{--}3 \mu\text{m}$. In all of these cases we find $\beta_i \sim 1$ and thus transport is in the realm where diffusion and surface kinetics are both significant.

Why is it that for the fastest experimentally determined surface reaction rates (corresponding to an accommodation coefficient of 0.7), the transport is not diffusion limited? As we now demonstrate, this is due to the fact that the radii of typical atmospheric aerosol particles are not much larger than the mean free path of the diffusing species. Let us evaluate $\beta \sim D/kR_p$ for transport of hypothetical condensible molecules to and from an aerosol particle. The diffusivity can be approximated by $D = \lambda_{i, \text{air}} \bar{c}_i^{3/2} (1 + (M_i/M_{\text{air}}))$ (Flagan and Seinfeld, 1988), where $\lambda_{i, \text{air}}$ is the mean free path of molecules of species i in air, \bar{c}_i is the mean speed of molecules of species i , M_i is the molecular weight of species i , and M_{air} is the mean molecular weight of air. We can relate the mean free path of a dilute species i in air to the mean free path of air molecules in air by $\lambda_{i, \text{air}} = \lambda_{\text{air}} \sqrt{2M_{\text{air}} / (M_i + M_{\text{air}})} (\sigma_{\text{air}}^2 / \sigma_{i, \text{air}}^2)$, where σ_{air} is the collision diameter for air molecules with each other and $\sigma_{i, \text{air}}$ is the collision diameter for molecules of species i with air molecules (Adamson, 1979). The rate constant can be expressed in terms of the mean molecular speed by $k = \alpha \bar{c}_i$ for condensation on aqueous-phase particles, where α is the accommodation

coefficient (Moore, 1972). For condensation on solid particles an appropriately weighted mean speed is used. Combining gives

$$\beta \sim \frac{\lambda_{\text{air}}}{\alpha R_p} \frac{3\pi}{32} \sqrt{2 \frac{M_{\text{air}} + M_i}{M_{\text{air}}} \frac{\sigma_{\text{air}}^2}{\sigma_{i,\text{air}}^2}}$$

Since the mean free path of molecules in air at STP is about $0.065 \mu\text{m}$ and $\frac{3\pi}{32} \sqrt{2(M_{\text{air}} + M_i)/M_{\text{air}}} (\sigma_{\text{air}}^2/\sigma_{i,\text{air}}^2)$ is of order unity, we can evaluate β at STP to obtain

$$\beta \sim \frac{0.065 \mu\text{m}}{\alpha R_p}$$

For $10 \mu\text{m}$ particles and accommodation coefficient near unity, the transport is diffusion limited, $\beta \ll 1$. For $0.1 \mu\text{m}$ particles, this limit does not hold even for unity accommodation coefficient, since particles this small challenge the continuum approximation. Thus we see that since the size of fine aerosol particles ($0.1\text{--}1 \mu\text{m}$ radius) are about the same as the mean free path, λ_{air} , small deviations from unity in the accommodation coefficient of these particles can shift the transport out of the diffusion limited regime.

Whether transport is governed by molecular diffusion, surface accommodation, or both is not only central to determining the rate of mass transport; it also determines the distribution of condensate with respect to particle size. To first order, if condensation is diffusion limited, the distribution of condensate is proportional to the first moment of the aerosol size distribution, whereas, if the condensation is surface accommodation limited, the distribution of condensate is proportional to the second moment of the aerosol size distribution.

At this point, we have been able to simplify the continuity equations and boundary conditions such that they describe the essential physics and chemistry of the mass transport of volatile inorganics between the gas and aerosol phases. We will now solve these equations for the flux of the chemical species under consideration.

Mass transport between the gas and aerosol phases

The concentration profiles of $\text{NH}_3(\text{g})$ and $\text{HX}(\text{g})$ that satisfy the differential equations and the boundary conditions at infinity are

$$C_i = C_{i,\infty} - A_i \frac{R_p}{r}$$

where the A_i are arbitrary constants that depend on the boundary conditions at the particle surface.

Applying the boundary conditions for solid-phase particles gives

$$\begin{aligned} J_i &= 4\pi r^2 D_i \frac{dC_i}{dr} \\ &= 2\pi R_p \sqrt{D_{\text{NH}_3} D_{\text{HX}}} \bar{C} (\beta_{\text{NH}_4\text{X}(s)} + 1) \end{aligned}$$

$$\times \left[1 - \sqrt{1 - 4 \frac{C_{\text{NH}_3,\infty} C_{\text{HX},\infty} - K_{\text{NH}_4\text{X}(s)}}{\bar{C}^2 (\beta_{\text{NH}_4\text{X}(s)} + 1)^2}} \right]$$

where $J_i = J_{\text{NH}_3} = J_{\text{HX}}$.

Applying the boundary conditions for aqueous-phase particles gives the flux of ammonia as

$$\begin{aligned} J_{\text{NH}_3} &= 4\pi r^2 D_{\text{NH}_3} \frac{dC_{\text{NH}_3}}{dr} \\ &= 4\pi R_p D_{\text{NH}_3} \frac{(C_{\text{NH}_3,\infty} - C_{\text{NH}_3,e})}{\beta_{\text{NH}_3} + 1} \end{aligned}$$

and the flux of acid as

$$\begin{aligned} J_{\text{HX}} &= 4\pi r^2 D_{\text{HX}} \frac{dC_{\text{HX}}}{dr} \\ &= 4\pi R_p D_{\text{HX}} \frac{(C_{\text{HX},\infty} - C_{\text{HX},e})}{\beta_{\text{HX}} + 1} \end{aligned}$$

where $C_{i,e}$ signifies the equilibrium gas-phase concentration of NH_3 or HX at the particle surface. Algorithms for calculating $C_{i,e}$ are given in Stelson and Seinfeld (1982b) for an ammonium nitrate and nitric acid solution. For more complex solutions, the methods described in Pilinis and Seinfeld (1987) can be used.

These expressions allow us to calculate the fluxes of NH_3 and HX to a single particle. There are other considerations that may affect this mass flux, such as (1) surface heating due to the latent heat of condensation and (2) motion of the particle with respect to the background gas due to settling and turbulent shear. These processes have all been considered and can be shown to be negligible.

With these expressions for the single particle mass fluxes, we are now able to address the problems of determining the mass flux to a population of aerosol particles and thus assessing the ultimate distribution of ammonium salt condensate.

AEROSOL POPULATION MASS TRANSFER

We have derived expressions that describe the fluxes of $\text{NH}_3(\text{g})$, $\text{HNO}_3(\text{g})$ and $\text{HCl}(\text{g})$ between the background gas and a single aerosol particle. Using these expressions, we now address the question: what are the physical and chemical processes that govern the distribution of ammonium salt condensate over a size- and composition-dispersed aerosol? We approach this problem by first examining the time scales for equilibration between the gas-phase concentrations and those at the aerosol surface. Then we address the more qualitative question of when there is a preference for condensate to appear on one particle size instead of another.

Equilibrium between the vapor phase and a population of aerosol particles

As we have just shown, transport between the gas and aerosol phases is in part determined by the

concentrations of NH_3 and HX at the particle surface and these concentrations in the background gas. Let us examine the situation where at first these concentrations are in equilibrium and then the background concentrations are suddenly increased so that condensation ensues. In general, the gas-phase concentrations decrease and the concentrations at the particle surface increase until equilibrium is attained. The decrease in background concentrations is due to depletion of species from the gas phase as they condense. The characteristic time, τ_∞ , for the two phases (aerosol and gas) to equilibrate due to this depletion is proportional to the total flux of gas-phase species to the aerosol phase.

For solid-phase aerosol particles, the surface concentrations are constant and τ_∞ is the only relevant time scale for the relaxation to equilibrium. For aqueous-phase particles, the gas-phase concentrations at the surface of the particles may increase as condensation proceeds, and this increase also tends to equilibrate the two phases. This change in gas-phase concentrations at the surface of a particle is due to changes in the chemical composition of the particle as condensation proceeds. We assume here that the gas-phase particle surface concentrations respond rapidly to changes in particle composition (Seinfeld, 1986). The characteristic time, τ_p , for the two phases to equilibrate due to the increase in particle surface concentration is proportional to the total flux of gas-phase species to the aerosol phase and, in addition, to the chemical composition of the aerosol phase.

The magnitude of τ_p is related to the ability of the aerosol phase to absorb NH_3 and HX . For solid particles, this absorptive capacity is infinite, since as ammonium salts condense, the surface equilibrium concentrations remain constant. The absorptive capacity of aqueous-phase particles is dependent on the composition of the particles. For certain compositions, the absorptive capacity is infinite, but for other compositions the absorptive capacity is finite. In the next section, we relate the composition of aqueous-phase particles to their absorptive capacity. In the remainder of this section, we estimate the magnitude of these two time scales, τ_∞ and τ_p .

The evolution of the background gas-phase concentration, $C_{i,\infty}$ due to transport to a monodisperse aerosol can be described by

$$\frac{dC_{i,\infty}}{dt} = -NJ_i$$

where J_i is the single particle flux (which is defined in the previous section for both solid- and aqueous-phase particles), i is NH_3 or HX , and N is the number concentration of aerosol particles. The characteristic time for gas-phase concentrations to change in the presence of transport to solid- or aqueous-phase particles is

$$\tau_\infty \sim \frac{\beta + 1}{4\pi NR_p \bar{D}}$$

where \bar{D} is an average diffusivity of the gas-phase species.

For solid aerosol particles, the surface concentrations remain constant as condensation proceeds and thus τ_p is irrelevant. For aqueous-phase particles, the surface concentration of condensing species may or may not change as condensation proceeds. In the next section we will discuss the cases where (1) water and ammonium salt condense on particles together to maintain constant molality and (2) the water content of the particle remains constant so that the molality changes during condensation. At this juncture, it is sufficient to state that both of these cases exist, but particle surface concentrations change most if the particle water content remains constant as inorganic species condense. In this case, the evolution of the liquid-phase molality, m_i , is given by

$$\frac{dm_i}{dt} \sim \frac{1}{m_w} NJ_i$$

where m_w is the liquid water mass of aerosol per unit volume of air.

The gas-phase surface equilibrium concentration, $C_{i,e}$, is related to the liquid-phase molality by an equilibrium constant, K_i (kg m^{-3}), which is a function of the composition of the particle and the ambient temperature, such that $C_{i,e} = K_i \gamma_i m_i$, where γ_i is the activity coefficient for species i . For activity coefficients of order unity, we obtain

$$C_{i,e} \sim K_i m_i.$$

Combining these two expressions gives an equation describing the evolution of the gas-phase surface equilibrium concentrations

$$\frac{dC_{i,e}}{dt} \sim \frac{K_i}{m_w} NJ_i,$$

and thus we find the characteristic time for the aqueous and gas phases to equilibrate due to changes in the gas-phase surface concentration is

$$\tau_p = \frac{m_w}{K_i} \tau_\infty.$$

In the derivation of this expression for τ_p , we assume the water content of the aerosol is not affected by condensation of the inorganics. If the water content increases with condensation, the surface concentrations will not change as rapidly, and τ_p will be larger.

We can express both time constants in terms of the mass of aerosol per unit volume of air, $m_p = 4/3 \pi R_p^3 \rho_p N$, if we make the assumption that aqueous-phase particles are mostly water, that is $m_w \sim m_p$. This assumption is best for dilute aerosol particles that occur under conditions of high relative humidity and may be off by at most a factor of 5 for highly concentrated particles that occur under conditions of low relative humidity. Note that if the relative humidity drops so low that $\text{NH}_4\text{X}(s)$ condenses, τ_p is no longer a relevant time constant. The restated time

constants are then

$$\tau_{\infty} = \frac{\rho_p R_p^2}{3D_i m_p} (\beta_i + 1)$$

and

$$\tau_p = \frac{\rho_p R_p^2}{3D_i K_i} (\beta_i + 1).$$

Notice that τ_{∞} is not dependent on the thermodynamic parameter K_i , but only on the transport parameters R_p and D_i , whereas τ_p is dependent on the thermodynamic parameter K_i in addition to the transport parameters. Qualitatively, τ_{∞} is the time scale for the gas and aerosol phases to equilibrate due to transport, whereas τ_p is the corresponding time scale due to thermodynamics. In the next section we will relate the relative magnitude of these time scales to whether transport or thermodynamics is the primary process that governs the distribution of ammonium salt condensate with respect to particle size. Let us now evaluate these time scales for some typical atmospheric conditions.

The ranges of these time constants are explored in Figs 3 and 4. The gas-phase time constant, τ_{∞} , is primarily a function of the mean particle radius and the aerosol mass concentration, and ranges from as little as a few seconds under conditions of high aerosol mass concentration and small mean radius to more than 1 day for low mass concentration and large particle radius. The particle surface time constant, τ_p , is primarily a function of the mean particle radius and temperature, since for $\text{NH}_4\text{Cl}(\text{aq})$ or $\text{NH}_4\text{NO}_3(\text{aq})$ the equilibrium constant varies by many orders of magnitude over the range of typical atmospheric temperatures. The equilibrium constant used in Fig. 4 is $\sqrt{K^*}$ of Stelson and Seinfeld (1982a) for

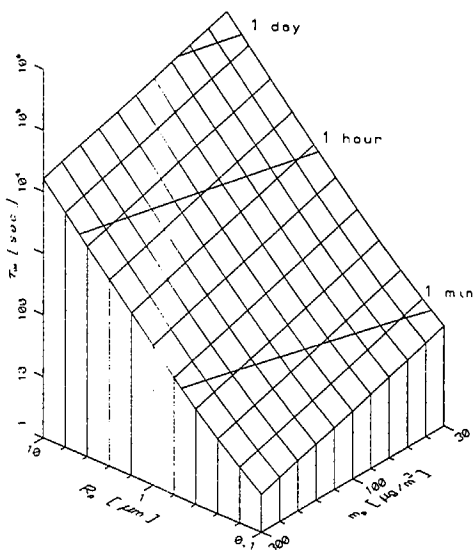


Fig. 3. The vapor phase time constant as a function of aerosol mass concentration and mean radius for NH_3 at 298 K and $\alpha=0.1$.

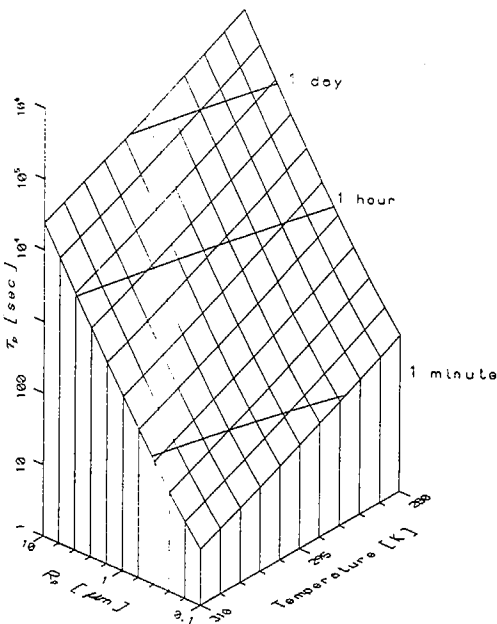


Fig. 4. The particle surface concentration time constant as a function of ambient temperature and mean aerosol radius for NH_3 in aqueous phase particles and $\alpha=0.1$.

$\text{NH}_4\text{NO}_3(\text{aq})$, and from this figure we see that τ_p ranges from a few seconds for high ambient temperatures and small mean aerosol radius to over 1 day for low ambient temperatures and large mean radius. The ambient temperature and aerosol mass concentration govern how the magnitude of τ_{∞} compares to that of τ_p . As will be discussed further in the next section, the relative size of these time scales is one factor that determines whether equilibrium or transport considerations govern the size distribution of ammonium salt condensate.

Two limiting cases may be identified from these figures for a location such as Los Angeles. Under coastal conditions (cool, low aerosol mass concentrations, and primary aerosol sizes), $\tau_{\infty} \sim \tau_p > 30$ h, and the aerosol surface concentrations are not necessarily in equilibrium with the gas phase. Under inland conditions (hot, high aerosol mass concentrations, and small aerosol sizes), $\tau_{\infty} \sim \tau_p \sim 4$ s, and equilibrium between the gas and aerosol phases is reached rather quickly. It is noteworthy that the data supporting thermodynamic equilibrium between the gas and aerosol phases were gathered at inland locations (Doyle *et al.*, 1979; Stelson *et al.*, 1979). In fact, our estimate of these time constants generally supports and is supported by the calculations and data of Russell and Cass (1986) and others that have focused on the inland conditions just described. Even if the particle is coated by surface active organics that result in an accommodation coefficient of $1/500$, τ_{∞} is still less than about 5 min.

For inland conditions, therefore, the assumption of equilibrium between the gas and aerosol phases is

evidently valid. Under other conditions, and especially those in Los Angeles coastal regions, the two phases are predicted not to be in equilibrium, and transport considerations will govern the distribution of condensate over particle size. In the next section, we will demonstrate that even under conditions where equilibrium is attained rapidly, equilibrium considerations do not always uniquely determine the distribution of condensate with respect to particle size.

Thermodynamics is not enough

In this section we explore in more detail the question of when thermodynamic considerations determine the distribution of ammonium salt condensate over particle size. The conclusion that will be reached is that under some conditions thermodynamics dominates, under other conditions transport dominates, and there is a range of cases where both play a role. Thus, a full description of the thermodynamic and transport properties of the aerosol population must be used to determine the distribution of ammonium salt condensate over particle size.

A number of assumptions are useful in the analysis that follows. First, the water content of the aerosol is assumed to be in instantaneous thermodynamic equilibrium with the environment, such that the activity of the liquid water is always equal to the relative humidity. Second, the water content of the atmosphere is much larger than the water content of the aerosol, so that the ambient relative humidity is assumed to be unaffected by condensation of inorganics and water on the aerosol. Both of these assumptions can be justified by the fact that the mass concentration of water vapor is much larger than the mass concentration of inorganic species under even the most polluted conditions.

Third, of the five prevalent inorganic compounds—sodium, ammonia, nitrate, sulfate and chlorine—sodium and sulfate are not volatile. Thus the primary concern is with condensation and evaporation of NH_3 , HCl and HNO_3 . And fourth, the Kelvin effect can be ignored, since in the range of particle radii of interest, 0.1–10 μm , the Kelvin effect plays a small role (Seinfeld, 1986).

When the aerosol is in thermodynamic equilibrium with the environment, the concentrations of the volatile inorganics at the surface of the particle must be equal to the concentrations of these species in the atmosphere. By extension, two aerosol particles of different size or composition are in thermodynamic equilibrium with each other if the concentrations at their surfaces are equal. Condensation on aerosol particles is proportional to the difference between the particle surface equilibrium gas-phase concentrations and the background concentrations, as well as the molecular diffusivity of the condensing species, the size of the particles, and the surface reaction rate constant. If two particles have identical surface equilibrium concentrations, the partitioning of condensate be-

tween the particles is governed by transport considerations. However, if two particles have different equilibrium surface concentrations, thermodynamics may govern the partitioning of condensate between them. Let us examine the cases where thermodynamics does and does not play a role in this partitioning.

When the ambient relative humidity is sufficiently low, the aerosol is a solid, and the product of the surface concentrations, $C_{\text{NH}_3} C_{\text{HCl}}$ and $C_{\text{NH}_3} C_{\text{HNO}_3}$, is identical for all particles, independent of size. Thus, the driving force is identical for all solid particles, the distribution of condensate over particle size is determined solely by transport considerations, and thermodynamic equilibrium plays no role.

Under conditions of intermediate relative humidity, the aerosol may consist of both an aqueous phase and an $\text{NH}_4\text{X}(\text{s})$ phase. If we assume these two phases to be in equilibrium, the product of the particle surface concentrations is governed by the existence of the solid. Thus, the presence of solid inclusions in an otherwise aqueous phase is thermodynamically identical to a solid phase.

Under conditions of sufficiently high relative humidity, the aerosol is an aqueous solution. For simplicity, let us consider the dissolution of one species, NH_4X . Thermodynamics plays more or less of a role in the distribution of NH_4X over particle size depending on how *osmotically dominant* NH_4X is in the aerosol solution. NH_4X is termed osmotically dominant when the concentration of NH_4X in the aerosol is much greater than the concentration of the other species. In this case, the amount of NH_4X in the aerosol controls the amount of water in the aerosol. (This is only true for relative humidities less than 100%; we are not considering fogs or clouds in this analysis.) This concept can be clarified by considering the ZSR expression used to calculate the water content of aerosol (Pilinis and Seinfeld, 1987):

$$\sum_i \frac{m_i}{m_{0,i}(\text{r.h.})} = 1$$

where m_i is the molality of electrolyte i and $m_{0,i}$ is the molality of electrolyte i such that the water activity is equal to r.h. in a solution whose only electrolyte is i . The molality can be expressed in terms of the moles of electrolyte i in the droplet divided by the mass of water in the droplet, $m_i = \hat{M}_i/W$, so that the expression above can be rewritten as

$$W = \frac{\hat{M}_{\text{NH}_4\text{X}}}{m_{0,\text{NH}_4\text{X}}(\text{r.h.})} + \sum_{i \neq \text{NH}_4\text{X}} \frac{\hat{M}_i}{m_{0,i}(\text{r.h.})}$$

where we have broken out the NH_4X term.

If $\hat{M}_{\text{NH}_4\text{X}}/m_{0,\text{NH}_4\text{X}}(\text{r.h.}) \gg \sum_{i \neq \text{NH}_4\text{X}} \hat{M}_i/m_{0,i}(\text{r.h.})$, NH_4X is osmotically dominant, the particle water content is governed almost completely by the mass of NH_4X in the particle, and thus $m_{\text{NH}_4\text{X}} = m_{0,\text{NH}_4\text{X}}(\text{r.h.})$. As NH_4X dissolves in the particle, water condenses in order to maintain the water activity identical to the atmospheric relative humidity, and thus the molality of

NH_4X is constant and equal to $m_{0,\text{NH}_4\text{X}}$ (r.h.). Therefore, if a population of size-distributed particles, osmotically dominated by NH_4X and in thermodynamic equilibrium with each other and the gas phase, is exposed to new gas-phase concentrations of NH_3 and HX , the size distribution of the condensate (or evaporate) is governed only by transport considerations, since the thermodynamic driving force between the gas and aerosol phases is identical for all particles osmotically dominated by NH_4X . Note that a particle can have at most one osmotically dominant species.

In the opposite limit, the mass of NH_4X is low compared to other solutes— NH_4X is *osmotically benign*, $\bar{M}_{\text{NH}_4\text{X}}/m_{0,\text{NH}_4\text{X}}(\text{r.h.}) \ll \sum_{i \neq \text{NH}_4\text{X}} M_i/m_{0,i}$ (r.h.)—and the water content of the particle is not affected by small changes in the particle NH_4X mass content. Here we find that the molality of NH_4X is roughly proportional to the mass of NH_4X dissolved, and thus the surface concentrations of the components of NH_4X reflect the mass of NH_4X in the particle. When NH_4X is osmotically benign, thermodynamics may govern its distribution over particle size, since the mass of NH_4X in the aerosol is reflected in the equilibrium surface concentrations and thus affects the driving force.

Let us now relate the previous time scale analysis and the osmotic dominance of an ammonium salt to the salt's distribution with respect to particle size. If the salt is osmotically dominant, the surface concentrations do not change as condensation proceeds and, as with solid aerosol particles, the particle characteristic time, τ_p , is irrelevant. As we have shown, transport considerations govern the distribution of NH_4X with respect to particle size for (1) particles that contain $\text{NH}_4\text{X}(\text{s})$ and (2) aqueous-phase particles osmotically dominated by $\text{NH}_4\text{X}(\text{aq})$.

For an osmotically benign ammonium salt, whether transport, thermodynamics, or a combination of the two governs the distribution of ammonium salt is dependent on the relative magnitudes of τ_∞ and τ_p . Imagine a population of aerosol particles in equilibrium with the surrounding gas. At time $t=0$, the gas-phase concentrations are suddenly increased in order to promote condensation. On the one hand, if $\tau_p \ll \tau_\infty$, the particle surface concentrations change until $t \sim \tau_p$, when they have come into equilibrium with the atmospheric concentrations and each other. During this equilibration, the gas-phase concentrations do not change significantly, because τ_∞ is large. Since the particles are in equilibrium, thermodynamic considerations govern the distribution with respect to particle size.

On the other hand, if $\tau_p \gg \tau_\infty$, the background concentrations adjust considerably faster than the particle concentrations until $t \sim \tau_\infty$, when the background concentrations come into equilibrium with the average gas-phase particle surface concentrations. Since τ_p is long compared to τ_∞ , the particle surface concentrations do not have time to change, and we conclude that transport considerations alone have

thus far governed the distribution of condensate. At this point, the particle surface concentrations, averaged over the aerosol population, are in equilibrium with the gas-phase concentrations, but particles of different size or composition may not be in equilibrium with each other. For $t > \tau_\infty$, these different aerosol particles tend to equilibrate, until $t \sim \tau_p$ when they reach a state of mutual equilibrium and thermodynamic considerations govern the distribution of condensate.

In conclusion, we find that transport considerations govern the distribution of condensate with respect to particle size for (1) solid particles; (2) an osmotically dominant ammonium salt in aqueous-phase particles, and (3) osmotically benign ammonium salts in aqueous-phase particles under the conditions just outlined. Otherwise, thermodynamic considerations or a combination of thermodynamic and transport considerations must be taken into account when distributing condensate over a size- and composition-dispersed aerosol population.

ACCURACY OF THE PREDICTED SIZE DISTRIBUTION

We have demonstrated that thermodynamics and transport both determine the distribution of ammonium salt condensate over a size-distributed aerosol. Furthermore, we have derived the governing equations for the flux of gas-phase species to a particle of a given composition. In this section, we examine the accuracy that we might expect to achieve in predicting the distribution of ammonium salt condensate over particle size.

There are three factors that determine the size distribution of condensing inorganics. First, the size and composition of the particles determine the magnitude of the Kelvin effect, which provides a thermodynamic driving force that moves NH_4X from smaller particles to larger ones.

Second, if particles of a given size have a uniform composition, the difference in composition between different size particles establishes a thermodynamic driving force between them. If, however, particles of a given size have very different compositions, there is also a thermodynamic driving force between particles of the same. In either case, particle composition affects the distribution of condensate via changes in the surface equilibrium concentrations.

Third, the surface rate constants not only govern the rate at which condensation and evaporation occur, but also the moment of the size distribution that determines the placement of the ammonium salts in the size spectrum. These rate constants are not well known under atmospheric conditions due to the limited data on the effective accommodation coefficient of surface active chemical species and which of these species are adsorbed on aerosols under different atmospheric conditions.

Ultimately, the model of the condensation of ammonia, nitric acid, and hydrochloric acid on aerosols that we have developed here will need to be incorporated into trajectory (Pilinis *et al.*, 1987) and Eulerian (Pilinis and Seinfeld, 1988) models of urban and regional scale air pollution. In previous work, the assumption is made that the composition of aerosol particles of a given size is uniform (Pilinis and Seinfeld, 1988). In addition to this approximation, there are inherent uncertainties in how well we can determine thermodynamic and physical properties of the aerosol population. In light of these approximations and uncertainties, we expect some uncertainty in the predicted size distribution of ammonium salt condensate. We will now estimate the source and magnitude of these uncertainties.

The Kelvin effect

The chemical potential of a species in a spherical aerosol particle, μ_p , can be related to its chemical potential in the bulk phase, μ_b , by the Gibbs-Thompson equation

$$\mu_p = \mu_b + \frac{2\sigma v}{R_p}$$

where σ is the surface tension and v is the molar volume of the species. For a pure particle, the Kelvin effect serves to increase the equilibrium partial pressure over the particle by a factor of $\exp(2\sigma v/RTR_p)$. For a solution droplet, the Kelvin effect tends to decrease the equilibrium water activity below the atmospheric r.h. by this factor while increasing the equilibrium solute vapor pressure by this factor. In this section we examine the magnitude of the Kelvin effect.

Uncertainties in the magnitude of the Kelvin effect arise primarily because of a lack of surface tension data. In general, surface tension data are available for aqueous solution droplets and solid NH_4Cl or NH_4NO_3 particles in a vacuum. We assume that these surface tension values are applicable under atmospheric conditions in spite of the fact that atmospheric

constituents adsorbed onto the particle surface would tend to lower its surface tension (Gill *et al.*, 1983).

Table 2 shows the value of $2\sigma v/RTR_p$ for various particle compositions and sizes. Since these values are all significantly less than unity, we can expand the exponential in a Taylor series and retain the first two terms to obtain $\exp(2\sigma v/RTR_p) \sim 1 + 2\sigma v/RTR_p$, so that $2\sigma v/RTR_p$ is approximately the change in surface partial pressures due to the Kelvin effect. If the Kelvin effect is taken into account, equilibrium is reached for solid particles when the volatile species have evaporated from the smaller particles and condensed on the largest ones. For aqueous solution particles, a volatile osmotically dominant species evaporates along with water until another species becomes osmotically dominant. This may substantially affect the size distribution of the aerosol, depending on the time scales involved. We expect that the surface tension may be uncertain by as much as 20%, so that from Table 2 we see that errors in surface equilibrium concentrations due to errors in the evaluation of the Kelvin effect may be as high as 3% but are usually less than 1%.

Surface equilibrium concentrations

Errors in the size distribution of condensate may result from the approximation that the volatile inorganic composition of the aerosol in a size range is uniform if in reality it is not. We might expect that non-volatile inorganics may not be uniformly distributed within a size range, but that the distribution of volatile species should be relatively uniform. We assume that this is the case and that errors in the surface equilibrium concentrations are due to inaccuracies in the calculation of the thermodynamic properties of the aerosol.

To assess the effect of these inaccuracies, let us examine the rate of NH_4X mass transfer between two arbitrary particle sizes. In the case of an aerosol containing solid NH_4X , the surface concentrations are determined by the equilibrium constant, which is independent of particle size or composition. When the

Table 2. Kelvin effect at 300 K

Particle composition	Molality (mol kg ⁻¹)	σ (ergs cm ⁻²)	v (ml mol ⁻¹)	$R_p = 0.03 \mu\text{m}$	$R_p = 0.1 \mu\text{m}$
				$\frac{2\sigma v}{RTR_p}$	$\frac{2\sigma v}{RTR_p}$
$\text{NH}_4\text{Cl(s)}$	—	80*	36§	0.07	0.03
$\text{NH}_4\text{NO}_3(\text{s})$	—	120†	46§	0.15	0.05
Pure water	—	73‡	18§	0.04	0.01
$\text{NH}_4\text{Cl(aq)}$	0	73‡	36	0.07	0.02
$\text{NH}_4\text{Cl(aq)}$	6	80‡	36	0.08	0.02
$\text{NH}_4\text{NO}_3(\text{aq})$	0	73‡	48	0.09	0.03
$\text{NH}_4\text{NO}_3(\text{aq})$	6	78‡	26	0.05	0.02

* Average of values in Henry *et al.* (1983).

† Extrapolated from Shah and Roberts (1985).

‡ Pruppacher and Klett (1980).

§ Perry and Chilton (1973).

|| Interpolated from Perry and Chilton (1973).

particles are an aqueous solution and NH_4X is osmotically dominant, the surface concentrations are determined by the equilibrium constant and $m_{0,i}(\text{r.h.})$ which again is independent of particle size. Thus, in both cases, the mass transfer and the resulting misplaced condensate are small. It is fortunate that the solid and osmotically dominant cases are not greatly affected by errors in the surface concentrations. Since the surface concentrations in these two cases are insensitive to the quantity of NH_4X in a particle, large amounts of material could be erroneously transferred from one particle size to another.

For an osmotically benign species, errors especially in the ZSR relation and in the Bromley model (Pilinis and Seinfeld, 1987) can lead to erroneous transfer of NH_4X between different size particles. A 10% error is reasonable for the ZSR and Bromley methods, and we use this error estimate in conjunction with subsequent time scale analysis to estimate the effect on the predicted distribution of NH_4X with respect to particle size.

Surface kinetics

Although the accommodation coefficients and surface accommodation rate constants are not well known, they may not greatly affect the distribution of condensate. Under the coastal conditions that we described previously, the aerosol is most likely aqueous, coated with either a biogenic or anthropogenic surface active hydrocarbon. If all particle sizes have a similar coating of organic, their accommodation coefficients are similar and the condensation is proportional to the second moment of the size distribution. Under these conditions, condensation proceeds relatively slowly and thus absolute errors in the accommodation coefficients or relative errors between the accommodation coefficients of different size particles only affect the distribution of a small quantity of condensate.

Under inland conditions typical of Los Angeles, the condensation proceeds rapidly due to the shorter time scales. Here we expect the gas and aerosol phases to be in relative equilibrium and thermodynamic differences between the composition of particles to govern the distribution of condensate (rather than the surface rate coefficients).

Time scales for movement of condensate between particle sizes

Uncertainties in the surface tension or thermodynamic properties of aqueous-phase aerosols may result in uncertainties in the distribution of inorganic condensate. To quantify this latter uncertainty, we now examine the movement of condensate between different size ranges of particles:

$$\frac{d\hat{m}_j}{dt} = N_j J_{i,j} f_w M_i$$

where \hat{m}_j is the particle mass at size j , $J_{i,j}$ is the molar flux of species i to a particle of size j , M_i is the

molecular weight of species i , N_j is the number density of particles of size j , and f_w is the change in total aerosol mass due to condensation of the volatile inorganic. f_w accounts for the condensation of water that results from the condensation of the ammonium salt. For solid particles or an osmotically benign species in aqueous particles, f_w is about one since the mass of water in these particles does not change significantly during condensation, however, for the osmotically dominant species,

$$f_w \sim 1 + \frac{1000}{m_{0,\text{NH}_4\text{X}}(\text{r.h.})M_{\text{NH}_4\text{X}}}$$

The molar flux can be expressed in terms of the concentration difference by $J_{i,j} \sim 4\pi D_i R_{p,j} \Delta C_i / (\beta_i + 1)$. If the uncertainty in surface concentration is the product of the background concentration and some factor, ϵ , then $\Delta C_i = \epsilon C_{i,\infty}$. The mass of aerosol in size range j can be expressed in terms of the particle radius, density, and number concentration by $m_j \sim 4/3 \pi R_{p,j}^3 \rho_p N_j$. Combining these expressions gives the characteristic time, τ_s , for movement of species i from one size particle to another

$$\tau_s \sim \frac{R_{p,j}^2 \rho_p (\beta + 1)}{3 D_{\text{NH}_4\text{X}} M_{\text{NH}_4\text{X}} \epsilon C_{\text{NH}_4\text{X},\infty} f_w}$$

Under coastal conditions, let us assume that $C_{i,\infty} \sim 1$ ppb and $f_w \sim 10$ since the aerosol is a dilute aqueous phase, which gives $\tau_s \sim 20$ days for $\epsilon = 0.1$. Thus, under coastal conditions, mass transfer between particles is so slow that a small error in surface concentrations has a small effect on the distribution of ammonium salt.

Under inland conditions, let us assume that $C_{i,\infty} \sim 50$ ppb and $f_w \sim 1$, which gives $\tau_s \sim 2$ min for $\epsilon = 0.1$. Errors in the surface tension or thermodynamics may be reflected in the predicted size distribution in only 2 min, whereas with $\epsilon = 0.01$, the error would take 20 min to be reflected in the distribution. Uncertainties in the surface tension do not seem to be reflected in significant uncertainties in the size distribution of ammonium salt condensate, since they are generally in the range of 1% or less. If under inland conditions the aerosol is in the solid phase, the surface partial pressures are well characterized and a 1% uncertainty is reasonable.

If the aerosol is a highly concentrated aqueous solution, the surface partial pressures of the osmotically dominant species are predicted fairly accurately, but we would not expect 1% accuracy for an osmotically benign species or a species of intermediate osmotic impact. Fortunately, these species do not comprise a large fraction of the total aerosol mass (since they are not osmotically dominant), and, although we expect some error, this error will not have a large impact on the total mass in a given size range. The largest uncertainties in the distribution probably occur under conditions of moderate humidity such that the aerosol is a highly concentrated solution, but such that there

is a substantial fraction of the smaller size particles. Under these circumstances, τ_s is small and the surface concentrations of all but the osmotically dominant species are poorly defined.

CONCLUSIONS

Over the past decade, a number of investigators have estimated the quantity of ammonium salt in atmospheric aerosol by assuming that chemical equilibrium exists between NH_4Cl and NH_4NO_3 in the aerosol phase and NH_3 , HCl and HNO_3 in the gas phase. We have undertaken a theoretical analysis of the chemical and physical processes that govern the formation of these aerosol ammonium salts and find that the time scales for the gas and aerosol phases to equilibrate depend crucially on the ambient conditions and the composition and state of the aerosol. In particular, these characteristic times are too long to justify the equilibrium assumption under cool ambient conditions or when the aerosol particles are large. Allen *et al.* (1989) find departures from equilibrium under cool conditions or under conditions of higher r.h. (when the particles are expected to be large due to increased water content) in agreement with our predictions.

Whether there is a thermodynamic preference for ammonium salt condensate to appear in one size particle over another depends on the state of the condensed ammonium salt (aqueous or solid), the osmotic dominance of the ammonium salt if it exists in the aqueous phase, and the relative magnitude of the time scales for the aerosol and the gas phase to equilibrate if the ammonium salt is not osmotically dominant. Thus an accurate prediction of the quantity of ammonium salt in atmospheric aerosol and its distribution with respect to particle size can only be obtained by explicitly modeling the transport of NH_3 , HNO_3 and HCl between the gas and aerosol phases.

Acknowledgement—This work was supported by the State of California Air Resources Board under Agreement No. A932-054.

REFERENCES

- Adamson A. W. (1979) *A Textbook of Physical Chemistry*, p. 70. Academic, New York.
- Allen A. G., Harrison R. M. and Erisman J. (1989) Field measurements of the dissociation of ammonium nitrate and ammonium chloride aerosols. *Atmospheric Environment* **23**, 1591-1599.
- Andersen W. H., Bills K. W., Dekker A. O., Mishuck E., Moe G. and Schultz R. D. (1958) The gasification of solid ammonium nitrate. *Jet Propul.* **28**, 831-832.
- Bassett M. and Seinfeld J. H. (1983) Atmospheric equilibrium model of sulfate and nitrate aerosols. *Atmospheric Environment* **17**, 2237-2252.
- Bassett M. and Seinfeld J. H. (1984) Atmospheric equilibrium model of sulfate and nitrate aerosols—II. Particle size analysis. *Atmospheric Environment* **18**, 1163-1170.
- Chaiken R. F., Sibbett D. J., Sutherland J. E., Van de Mark D. K. and Wheeler A. (1962) Rate of sublimation of ammonium halides. *J. chem. Phys.* **37**, 2311-2318.
- Clementi E. and Gayles J. N. (1967) Study of the electronic structure of molecules. VII. Inner and outer complex in the NH_4Cl formation from NH_3 and HCl . *J. chem. Phys.* **47**, 3837-3841.
- Countess R. J. and Hecklen J. (1973) Kinetics of particle growth. II. Kinetics of the reaction of ammonia with hydrogen chloride and the growth of particulate ammonium chloride. *J. phys. Chem.* **77**, 444-447.
- Dahlin R. S., Su J. and Peters L. K. (1981) Aerosol formation in reacting gases: theory and application to the anhydrous NH_3 - HCl system. *AIChE J.* **27**, 404-418.
- de Kruijff C. G. (1982) The vapor phase dissociation of ammonium salts: ammonium halides, ammonium rhodanide, ammonium nitrate, and ammonium bicarbonate. *J. chem. Phys.* **77**, 6247-6250.
- Doyle G. J., Tuazon E. C., Graham R. A., Mischke T. M., Winer A. M. and Pitts J. N. (1979) Simultaneous concentrations of ammonia and nitric acid in a polluted atmosphere and their equilibrium relationship to particulate ammonium nitrate. *Envir. Sci. Technol.* **13**, 1416-1419.
- Flagan R. C. and Seinfeld J. H. (1988) *Fundamentals of Air Pollution Engineering*. Prentice Hall, Englewood Cliffs, NJ.
- Gelbard F., Tambour Y. and Seinfeld J. H. (1980) Sectional representation for simulating aerosol dynamics. *J. Colloid Interface Sci.* **76**, 541-556.
- Gill P. S., Graedel T. E. and Weschler C. J. (1983) Organic films on atmospheric aerosol particles, fog droplets, cloud droplets, raindrops, and snowflakes. *Rev. Geophys. Space Phys.* **21**, 903-920.
- Graedel T. E., Gill P. S. and Weschler C. J. (1983) Effects of organic surface films on the scavenging of atmospheric gases by raindrops and aerosol particles. In *Precipitation Scavenging, Dry Deposition, and Resuspension* (edited by H. R. Pruppacher, R. G. Semonin and W. G. N. Slinn), pp. 417-430. Elsevier Science, New York.
- Gray H. A., Cass G. R., Huntziger J. J., Heyerdahl E. K. and Rau J. A. (1986) Characteristics of atmospheric organic and elemental carbon particle concentrations in Los Angeles. *Envir. Sci. Technol.* **20**, 580-589.
- Grosjean D. (1982) The stability of particulate nitrate in the Los Angeles atmosphere. *Sci. total Envir.* **25**, 263-275.
- Heintzenberg J. (1989) Fine particles in the global troposphere. A review. *Tellus* **41B**, 149-160.
- Henry J. F., Gonzalez A. and Peters L. K. (1983) Dynamics of NH_4Cl particle nucleation and growth at 253-296 K. *Aerosol Sci. Technol.* **2**, 321-339.
- Hightower R. L. and Richardson C. B. (1988) Evaporation of ammonium nitrate particles containing ammonium sulfate. *Atmospheric Environment* **22**, 2587-2591.
- Hildemann L. M., Russell A. G. and Cass G. R. (1984) Ammonia and nitric acid concentrations in equilibrium with atmospheric aerosols: experiment vs theory. *Atmospheric Environment* **18**, 1737-1750.
- Hill C. G. (1977) *An Introduction to Chemical Engineering Kinetics and Reactor Design*. Wiley, New York.
- Moore W. J. (1972) *Physical Chemistry*. Prentice-Hall, Englewood Cliffs, New Jersey.
- Perry R. H. and Chilton C. H. (1973) *Chemical Engineers' Handbook*. McGraw-Hill, New York.
- Pilinis C. and Seinfeld J. H. (1987) Continued development of a general equilibrium model for inorganic multicomponent atmospheric aerosols. *Atmospheric Environment* **21**, 2453-2466.
- Pilinis C. and Seinfeld J. H. (1988) Development and evaluation of an Eulerian photochemical gas-aerosol model. *Atmospheric Environment* **22**, 1985-2001.
- Pilinis C. and Seinfeld J. H. and Seigneur C. (1987) Mathematical modeling of the dynamics of multicomponent atmospheric aerosols. *Atmospheric Environment* **21**, 943-955.

- Pio C. A. and Harrison R. M. (1987) Vapour pressure of ammonium chloride aerosol: effect of temperature and humidity. *Atmospheric Environment* **21**, 2711-2715.
- Pruppacher H. R. and Klett J. D. (1980) *Microphysics of Clouds and Precipitation*. Reidel, Holland.
- Ramsay W. and Young S. (1886) On evaporation and dissociation. *Phil. Trans. R. Soc. London* **177**, 71-122.
- Richardson C. B. and Hightower R. L. (1987) Evaporation of ammonium nitrate particles. *Atmospheric Environment* **21**, 971-975.
- Rodebush W. H. and Michelak J. C. (1929) The vapor pressure and vapor density of intensively dried ammonium chloride. *J. Am. Chem. Soc.* **51**, 748-759.
- Russell A. G., McRae G. J. and Cass G. R. (1983) Mathematical modeling of the formation and transport of ammonium nitrate aerosol. *Atmospheric Environment* **17**, 949-964.
- Russell A. G. and Cass G. R. (1986) Verification of a mathematical model for aerosol nitrate and nitric acid formation and its use for control measure evaluation. *Atmospheric Environment* **20**, 2011-2025.
- Russell A. G., McCue K. F. and Cass G. R. (1988) Mathematical modeling of the formation of nitrogen-containing air pollutants. 1. Evaluation of an Eulerian photochemical model. *Environ. Sci. Technol.* **22**, 263-271.
- Saxena P., Hudischewskyj A. B., Seigneur C. and Seinfeld J. H. (1986) A comparative study of equilibrium approaches to the chemical characterization of secondary aerosols. *Atmospheric Environment* **20**, 1471-1483.
- Saxena P., Seigneur C. and Peterson T. W. (1983) Modeling of multiphase atmospheric aerosols. *Atmospheric Environment* **17**, 1315-1329.
- Schultz J. S., Goddard J. D. and Suchdeo S. R. (1974) Facilitated transport via carrier-mediated diffusion in membranes. *AIChE J.* **20**, 417-444.
- Schultz R. D. and Dekker A. O. (1956) The effect of physical adsorption on the absolute decomposition rates of crystalline ammonium chloride and cupric sulfate trihydrate. *J. phys. Chem.* **60**, 1095-1100.
- Seinfeld J. H. (1986) *Atmospheric Chemistry and Physics of Air Pollution*. Wiley, New York.
- Shah K. D. and Roberts A. G. (1985) Properties of ammonium nitrate. *Fert. Sci. Technol. Ser.* **4**, 171-197.
- Shibata S. (1970) Structure of gaseous ammonium chloride. *ACTA Chem. Scand.* **24**, 705-706.
- Smith A. and Lombard R. H. (1915) The densities and degrees of dissociation of the saturated vapors of the ammonium halides, and the related thermal data. *J. Am. Chem. Soc.* **37**, 38-70.
- Stelson A. W., Friedlander S. K. and Seinfeld J. H. (1979) A note on the equilibrium relationship between ammonia and nitric acid and particulate ammonium nitrate. *Atmospheric Environment* **13**, 369-371.
- Stelson A. W. and Seinfeld J. H. (1982a) Relative humidity and temperature dependence of the ammonium nitrate dissociation constant. *Atmospheric Environment* **16**, 983-992.
- Stelson S. W. and Seinfeld J. H. (1982b) Relative humidity and pH dependence of the vapor pressure of ammonium nitrate-nitric acid solutions at 25°C. *Atmospheric Environment* **16**, 993-1000.
- Stephenson C. C. (1944) The dissociation of ammonium chloride. *J. chem. Phys.* **12**, 318-319.
- Sturges W. T. and Harrison R. M. (1988) The evaporation of ammonium chloride aerosol. In *Aerosols. Their Generation, Behaviour, and Applications. Proc. of the Second Conference of the Aerosol Society, U.K.*, pp. 7-12.
- Tang S. P. and Fenn J. B. (1973) Vacuum sublimation of ammonium perchlorate. *J. phys. Chem.* **77**, 940-944.
- Tanner R. L. (1982) An ambient experimental study of phase equilibrium in the atmospheric system: aerosol H^+ , NH_4^+ , SO_4^{2-} , NO_3^- - $\text{NH}_3(\text{g})$, $\text{HNO}_3(\text{g})$. *Atmospheric Environment* **16**, 2935-2942.